



Pedological and hydrogeological setting and subsurface flow structure of the carbonate-rock CZE Hainich in western Thuringia, Germany

Bernd Kohlhepp¹, Robert Lehmann¹, Paul Seeber¹, Kirsten Küsel^{2,3}, Susan E. Trumbore⁴ and Kai U. Totsche¹

¹Hydrogeology, Institute of Geosciences, Friedrich Schiller University Jena, Burgweg 11, 07749 Jena, Germany

²Aquatic Geomicrobiology, Institute of Ecology, Friedrich Schiller University Jena, Dornburger Strasse 159, 07743 Jena, Germany

³German Centre for Integrative Biodiversity Research (iDiv), Halle-Jena-Leipzig, Deutscher Platz 5d, 04103 Leipzig, Germany

⁴Biogeochemical Processes, Max Planck Institute for Biogeochemistry Jena, Hans-Knöll-Str. 10, 07745 Jena, Germany

Correspondence to: Kai U. Totsche (kai.totsche@uni-jena.de)



Abstract

The quality of near surface groundwater reservoirs is to a large extent controlled by land use and the properties of the soils in the recharge areas. Studies on groundwater quality and vulnerability, therefore, call for a thorough and holistic analysis of the buildup and hydraulic properties of the full range of surface and subsurface compartments involved in the interactions of water with immobile surfaces of the soils and rocks. This study provides a comprehensive characterization of the soils sensu stricto, the unsaturated zone, aquifer stratigraphy and hydrochemistry in a hillslope karst environment of a carbonate-rock subcatchment of the Hainich Critical Zone Exploratory (CZE). This CZE is located within the Upper Muschelkalk Formations in the Hainich low mountain range, Thuringia, central Germany. We investigated the soils, surface geology, land use types and the infiltration properties based on a field survey. Aquifer stratigraphy, lithology and structure were analyzed based on drill core analysis, mineralogical analysis and geophysical borehole logs. Hydrogeochemical data from 15 permanent monitoring wells along a 5.4 km long hillslope transect were analyzed for major and minor ions, total and dissolved organic and inorganic carbon during a 4 year monitoring period and were statistically evaluated.

The geological succession of the interlayered and laterally continuous limestone (karst/) fracture aquifers and marlstone aquitards of the Upper Muschelkalk results in two main aquifer assemblages (HTL and HTU = Hainich transect lower/upper aquifer assemblage), which comprise ten previously undocumented individual aquifer storeys. The geologically inferred stratification of the subsurface was confirmed by principal component analysis and cluster analysis of groundwater chemistry. According to groundwater compositions within the HTL and HTU assemblages, there are 5 main clusters (2 in HTU and 3 in HTL). Soil properties are related to infiltration rates and the initial chemistry of recharge waters. The reconstructed recharge zones for the aquifer storeys are characterized by predominantly forest land use on “carbonate series” soils and cropland/pasture land use on “siliceous series” soils, the latter developed from quarternary aeolian loess and alluvial valley fills.

Based on the local geological structure, aquifers in the lower positions of the litho/hydrostratigraphy (i.e. HTL) outcrop in higher slope positions, show greater catchment sizes and a greater limestone/marlstone-ratio. The latter leads to thin soils, low water retention potential and predominantly forest land use, resulting in presumably high groundwater recharge rates and little anthropogenic influence on groundwater quality. As the subsurface stratification enforces confined groundwater flow, intrastratal karstification and the resulting hydraulic conductivity increases (and groundwater residence time decreases) with increasing bed thickness and limestone/marlstone ratio towards the lower portions of the stratigraphic succession. By implication, aquifers in the upper litho/hydrostratigraphic positions (HTU) exhibit small and partly agriculturally managed catchments with thick soils, low infiltration potential and, based on thinly bedded aquifer/aquitard successions, low hydraulic conductivities and long groundwater residence times. All in all, the complex interplay of geological structure, lithology, soil group and land use type results in distinct hydrochemical, and presumably ecological conditions in the different aquifers.

Keywords

critical zone, fractured rock aquifers, groundwater recharge, hydrostratigraphy, infiltration, intrastratal karst, lithostratigraphy, Muschelkalk, soils

Copyright statement

The authors grant, that they are authorized by their co-authors to enter into the following arrangements. The work described has not been published before (except in the form of an abstract or proceedings-type publication – including discussion papers – or as part of a published lecture or thesis). It is not under consideration for publication elsewhere, and its publication has been approved by all the authors and by the responsible authorities – tacitly or explicitly – of the institutes where the work was carried out. The authors have secured the right to reproduce any material that has already been published or copyrighted elsewhere. The authors agree to the following license and copyright agreement:



The copyright of any article is retained by the authors. Authors grant Copernicus Publications a license to publish the article and identify itself as the original publisher. Authors grant Copernicus Publications commercial rights to produce hardcopy volumes of the journal for purchase by libraries and individuals. Authors grant any third party the right to use the article freely under the stipulation that the original authors are given credit and the appropriate citation details are mentioned.

- 5 The article is distributed under the Creative Commons Attribution 3.0 License. Unless otherwise stated, associated published material is distributed under the same license.



1 Introduction

The holistic reconstruction of the subsurface architecture of carbonate-rock landscapes is mandatory to reveal their hydrogeological functioning for sustainable management and resource protection. The hydrogeochemical and (micro)biological compositions of shallow (< 200 m) groundwater bodies may be to a large extent controlled by the biogeochemical processes and the fluid-rock/soil interactions while traveling through the overburden of the aquifers (Urich, 2002; Canora et al., 2008). The subsurface compartments that form the overburden are (from surface to subsurface) (I.) the soils *sensu stricto*, i.e. the rather thin (< 1-2 m), pedogenetically transformed, intensively rooted and enlivened uppermost parts of the Earth's crust, (II.) the partly water saturated, weakly weathered to almost unaltered rocks, and finally (III.), the water saturated rocks that may act as aquifers, aquicludes or aquitards. Infiltrating rain water, as the main component of groundwater recharge, first passes the soils, which are a source for mobile organic carbon (Guggenberger and Kaiser, 2003), suspended particles (Münch et al., 2002; Totsche et al. 2006, 2007; Schrupf et al., 2013; Gleixner, 2013) and even biota (Dibbern et al., 2014) as well as for fertilizers (Köhler et al., 2006) and pesticides from agriculture (Müller et al., 2003). The residence time of the seepage water regulates the chemical and biological quality by controlling the extent to which the partial equilibrium of the rate-limited dissolution, retardation and release processes is achieved (Weigand and Totsche, 1998; Münch et al. 2002). Residence times depend on the duration and intensity of precipitation, moisture content, water retention characteristics and the presence of macropores. A number of papers present detailed studies of karst groundwater chemistry (Suk and Lee, 1999; Moore et al., 2009), of interactions between karst groundwater and springs (Barberá and Andreo, 2012), or they present structural karst aquifer models with the simulation of groundwater flow (Dafny et al., 2010), whereas the overlying soils are not considered in these studies. Other studies that focus on flow path models in the unsaturated zone (Pronk et al., 2009) or on water balance and groundwater recharge, consider land use and soil groups (Steward et al., 2011; Allocca et al., 2014) but without a detailed description of aquifer structure/stratigraphy. Some studies assess the aquifer vulnerability by considering unsaturated zone lithology and hydraulic conductivities (Witkowski et al., 2003), yet leaving groundwater chemistry out of focus. Up to now, a comprehensive characterization of the full range of surface and subsurface compartments, including the soils, the unsaturated zone and the detailed aquifer structure and stratigraphy is lacking. This holds in particular for karst landscapes that supply 25 % of the world's population with drinking water (Ford and Williams, 2007).

This study presents such a holistic analysis of the subsurface compartments of the Hainich CZE involved in subsurface water flow, connecting the surface (impacted by land use) with the groundwater bodies. This includes the reconstruction of the aquifer recharge areas, characterization and mapping of land use types, soils and surface geology (including karst and fracture zones), litho/hydrostratigraphic core characterization and geophysical borehole logs as well as the statistical analysis of the groundwater composition. The main aims of this study are (1) the characterization of subsurface architecture and flow paths, (2) the reconstruction and assessment of infiltration potential in the groundwater catchment, and (3) the influence of land use, soils, topography, lithology, geological structure and karstification on groundwater compositions. The results of this study provide the surface/subsurface framework and conceptual understanding of hydrochemistry for the Hainich CZE research site, which is unique for observing cultural landscapes on carbonate-rock aquifer systems in temperate climates (Küsel et al., 2016). The study is embedded within the collaborative research centre 1076 AquaDiva (www.aquadiva.uni-jena.de), that aims to explore the mutual dependency of the functional biodiversity of the subsurface compartments, controlled by land use, weather events, and especially on the role of the local geology for the functioning of the groundwater ecosystem (Küsel et al., 2016).



2 Material and methods

2.1 Site description

The Hainich CZE is part of the Hainich low mountain range and covers 430 km² of a hillslope subcatchment of the Unstrut River in northwestern Thuringia, Central Germany (Fig. 1). It is limited by the recipient stream (Unstrut River) and the distribution zones of the Upper Muschelkalk target formations. The NW-SE orientated Hainich ridge is a geological anticline that developed topographically as a low mountain range with a steep western, and a moderately inclined eastern flank (Jordan and Weder, 1995). The western flank of the Hainich is characterized by complex tectonics with NW-SE oriented grabens, bounded by normal faults that belong to the regionally important Eichenberg-Gotha-Saalfeld fault zone (Mempel, 1939; Patzelt, 1998). The eastern flank of the Hainich hillslope with the study area, shows a rather simple geostructural setup with NE dipping strata in the direction of the syncline of Mühlhausen-Bad Langensalza (Kaiser, 1905; König, 1930; Patzelt, 1998; Wätzel, 2007). Although little is known about the exact uplift and exhumation age, (NW-SE) fault orientations and the position between the two large horst structures Thüringer Wald and Harz (low mountain ranges), uplifted in the Late Cretaceous (Voigt et al. 2004; Kley and Voigt, 2008), point to a similar history of uplift of the Hainich ridge in the Late Cretaceous.

Groundwater flow is supposed to take place mainly in fractured hard rock aquifers and very subordinate in quaternary valley fills. The Hainich low mountain range is one of the regionally important recharge areas like the Dün, the Fahner Höhe or the Ettersberg in Thuringia (Fig. 1) and is also a typical example of peripheral groundwater supply for water deficient sedimentary basins (Rau and Unger, 1997; Hiekel, 2004). The area belongs to the Cfb climate region (C: warm temperate, f: fully humid, b: warm summer) according to the Köppen-Geiger classification (Kottek et al., 2006) and exhibits a leeward decline in areal precipitation and increasing mean air temperature from the Hainich ridge (> 900 mm/y; 7.5-8 °C) to the Unstrut valley (< 600 mm/y; 9-9.5 °C; long term average 1970-2010, Thüringer Landesanstalt für Umwelt und Geologie, 2016). The intensively investigated study area is limited to a 29 km²-subarea of the Hainich CZE, that surrounds the soil and groundwater monitoring transect (Küsel et al., 2016).

The AquaDiva transect consists of multiple wells at five sites for groundwater monitoring, termed H1 to H5. Each site contains 1 to 4 drilled wells labeled with a suffix, for instance H51, H52 and H53. Site H1 (wells H11 to 14) and H2 (H21 to H23) are located in the upper hillslope region of the catchment, which is covered by forest. Sites H3 (H31/32), H4 (H41 to H44) and H5 (H51 to H53) are situated in the agriculturally used, middle and lower slope regions of the Hainich hillslope (Fig. 1).

30

2.2 Data resources

Field survey

Characterization of the geological, hydrogeological and pedological situation as well as of the infiltration properties in the Hainich CZE was based on a field survey carried out in the intensively investigated subcatchment of the Unstrut River (Fig. 1). 482 outcrops were described within an area of 29 km² considering lithology (according to Dunham, 1962) and karst features. In the same area, a total of 117 soil profiles resulted from ramcore drillings (50 and 60 mm diameter), supplemented by 154 (Pürckhauer, 22 mm) soil profiles. Ramcore drilling was done with an electrically powered motor hammer (GSH 27, Robert Bosch GmbH, Germany) up to depths of 5 meters to reach the host rock. Soil mapping focuses on the influence of geology, relief and land use on infiltration properties. Soil description was carried out according to the German soil survey instruction (Bodenkundliche Kartieranleitung KA5, AG Boden, 2005) and the world reference base (WRB)-scheme (IUSS Working Group WRB, 2006). Soil colors were determined using a Munsell soil color chart. Outcrop mapping was supplemented by the description of rubblestones on cropland, for distinguishing underlying loess loam, marlstone, dolomite and limestone. Strike and dip directions were constructed, based on the boundary between the most



prominent limestone package (Trochitenkalk formation) and the superposing limestone-marlstone alternations (Meissner formation).

Analysis of drill cores and borehole logs

5 For the determination of the stratigraphic succession, aquifer properties and mineralogical indicators for groundwater flow, 395 meters of cores from twelve drillings were investigated. Core description, based on DIN EN ISO 14689-1 (geotechnical classification of rock) comprised hydrogeological features like fractures and pores and a weathering index. We extended it to sedimentary structures, limestone classification (Dunham, 1962), pore classification (Lucia, 1983), the degree of karstification, the aquifer type, fracture angles and fracture colors, as well as secondary mineralization on fractures, which are indicative for recent and past groundwater flow pathways. Additional information about stratigraphy, clay content, 10 fracturing and groundwater inflow was revealed by analyzing geophysical open-borehole logs of ten drillings from the upper to the lower slope (site H1/2/3/4/5, Fig. 1). This included data on caliper, passive gamma-ray radiation, sonic velocity (delay time of sound waves), specific electrical resistivity of rocks, as well as the temperature and specific electrical resistivity of well water. Gamma-ray curves are interpreted based on the graphical correlation of high gamma ray peaks (marlstones) and intersections of gamma ray curves with an empirically defined “shale line”, here at 90 API (separating limestones from 15 marlstones). The spatial correlation of marlstones presumes that basin centre marlstones are laterally more continuous than shallow water limestones (Aigner, 1985).

Rock forming minerals were analyzed on a Bruker D8 Advance X-ray diffractometer (XRD, Cu-K α -anode, 40 kV, 40 mA, Bruker AXS Inc., USA) and Fourier transform infrared spectroscopy (FTIR) on pressed powder samples with a Thermo 20 Fisher Scientific Nicolet iS10 device (wavenumber 4000 to 400 cm⁻¹, Thermo-Fisher Scientific, USA).

The two-dimensional correlation of geophysical and geological well logs was carried out with well management software GeoDIN V.8 (Fugro Consult GmbH, Germany). The scope of the correlation was to figure out lateral continuity of flow domains separated by aquitards for achieving information about potential modes of bedding-parallel, intrastratal and cross-formational fluid flow.

25

Hydrogeochemistry and hydraulics

Groundwater levels were recorded by permanently installed data loggers (Orpheus Mini, Ecolog 500/800, OTT Hydromet GmbH, Germany). Groundwater was sampled every four weeks over three hydrological years (Nov. 2013 to Oct. 2015) in 15 permanent monitoring wells (5.1 to 88.5 m final depth below surface) of five sites along the 5.4 km long well transect 30 (Fig. 1) between 417 and 244 meters above mean sea level (masl). The groundwater accessing wells were regularly sampled with submersible motor pumps (MP1, Grundfos, Denmark) or, in the case of very low water levels with bladder pumps/bailers. The physicochemical parameters temperature (T), pH, redox potential (Eh), electrical conductivity (temperature corrected at 25°C; EC-25) and dissolved oxygen (O₂) of groundwater samples were measured on site using a flow-through cell, probes for pH (SenTix 980, WTW GmbH, Germany; manufacturer for all probes mentioned), electrical 35 conductivity (TetraCon 925), redox potential (SenTix ORP 900), concentration of dissolved oxygen (FDO 925) and a multi-parameter meter (Multi 3430 IDS, WTW GmbH, Germany). Hydrochemical analyses (duplicates) comprised major and minor ions (< 0.45 μ m, PES filter) by ICP-OES (725 ES, Varian/Agilent, USA) and ICP-MS (Thermo Fisher Scientific, Germany; Thermo Electron, U.K.), acid and base neutralizing capacity by acid/base-titration, major anions (SO₄²⁻, Cl⁻, NO₃⁻, NO₂⁻, PO₄³⁻; PES filter < 0.45 μ m) by ion chromatography (DX-120, DIONEX, USA), redox sensitive parameters (Fe²⁺, 40 NO₂⁻, NH₄⁺, HS⁻) by colorimetry (DR/890, Hach, USA) and determination of carbon sum parameters (TOC, TIC, DIC, DOC; PES filter < 0.45 μ m) by high temperature catalytic oxidation (multi 18 N/C 2100S, AnalytikJena, Germany). Groundwater was classified using a Piper plot (Piper, 1944) according to Furtak and Langguth (1967) and Kralik et al. (2005).



Geospatial analysis and reconstruction of recharge areas

For the assessment of the major recharge areas, overlays of the compiled geological and soil maps with land use maps interpreted from field observations and aerial imagery, as well as a digital elevation model (DEM) with 2 m resolution were prepared using ArcGIS 10.3 (ESRI Inc., USA). The primary data sets were interpreted in terms of land use types, surface morphology and drainage patterns with special focus on karst phenomena like sinkholes, which are discussed in the literature as preferential input features for surface/rain water (Nennstiel, 1933; Mempel, 1939; Hecht, 2003). Owing to the local geology with geological strata inclined at an angle steeper than the hillslope, the area, position and land use types in the aquifer recharge zones can be reconstructed and preferential infiltration/recharge areas can be identified for each fractured limestone interval (potential aquifer).

Statistical analysis

SPSS 22 (IBM Corp., USA) and Origin Pro 2015 (OriginLab Corp., USA) were used for descriptive and multivariate statistics of the hydrochemical data. This includes hierarchical cluster analysis (HC) for distinguishing hydrogeochemical groups independently from geologically defined aquifer stratifications. Two different parameter sets were statistically examined at the same number of groundwater analysis from three hydrological years. A complete parameter set (a), including all measured parameters, was chosen to figure out control parameters influencing the hydrochemical compositions of the groundwater domains by means of Principal Component Analysis (PCA). As redox processes seems to be very distinct in the studied groundwaters (masking other processes), a limited parameter set (b) was defined that does not include ions which are strongly affected by redox processes. The complete parameter set (a) contains, EC-25, pH, dissolved oxygen, Eh, TOC, anions (NO_3^- , Cl^- , SO_4^{2-}), cations (Ca^{2+} , Mg^{2+} , Mn^{2+} and 4^+ , K^+ , Na^+ , Fe^{2+} and 3^+ , Zn^{2+} , Sr^{2+} , Ba^{2+}) and silica (Si^{4+}). The limited parameter set (b) includes EC-25, pH, Cl^- , Ca^{2+} , Mg^{2+} , K^+ , Na^+ , Zn^{2+} , Sr^{2+} , Ba^{2+} and Si^{4+} . Data preparation for HC includes a z-score normalization of concentrations. Strongly correlating variables (> 0.9) and constant values were excluded, outliers were eliminated (next neighbor method) and listwise deletion was carried out (Backhaus et al., 2016). Then, a euclidian distance measure was applied and five clusters were chosen based on the visual observation of the scree plot elbow criterion (Cattell, 1966). The phenon line was chosen at a linkage distance of about 67. Thus, samples with a linkage distance lower than 67 were grouped into the same cluster. Finally, Ward's method for clustering was applied (Ward, 1963).

3 Results

3.1 Landscape morphology, hydrography and land use

The study area covers altitude regions between 170 and 494 masl with an average slope of 35 m/km. The relief forms a stepless, gently inclined plane and is cut by more than ten straight, parallel and roughly equidistant SW-NE oriented oblique valleys with steeper upper slope angles in headwater areas. Karst phenomena like sinkholes (each of up to 80 m in diameter) are concentrated in a NW-SE oriented lineament at the middle Hainich hillslope (at about 355 masl). Sinkholes occur on local ridges and not in valleys. A second and parallel lineament of shallow elongated (uvala-like) karst depressions with a horizontal extent of up to 400 m crosses the lower Hainich hillslope (at about 270 masl).

The Hainich low mountain range is the topographic water divide with eastward discharge towards the Unstrut River and westward towards the Werra River. Only a few small contact springs occur in the study area, most of them coupled to boundaries between geological formations. Larger springs (for instance the springs coupled to the Kllstedter fault zone; Fig. 1) occur at the lower eastern slopes of the Hainich ridge, tracing regional fault/fracture zones. Headwater areas of creeks, small rivers, oblique valleys and even agricultural drainage ditches are mostly dry. During our monitoring period (November 2013 to May 2016) surface water runoff typically occurred from December to March.



Major land uses are agriculture (crop, pasture) and forest (unmanaged and managed deciduous forest). Forests are to a large extent within the unmanaged Hainich National Park that occupies ridge and upper- to mid-slope positions and dominate the southwestern portion of the study area. Areas within the Hainich National Park that had been formerly used as military tank training areas are now covered with uncultivated grassland/scrubland successions. Aerial images and digital elevation

5 models show parallel lanes, drainage trenches and plough-like traces, the latter from the clearance of ammunition. Cultivated grasslands outside the Hainich National Park, which are used both as meadows and pastures, cover parts of the middle slope and locally some cleared glades at the upper slope as well as riparian areas of small rivers. Cropland (locally used for wheat, corn and canola production) covers mainly the middle and lower slopes (Fig. 2).

10 3.2 Land use history

As we assume that the land use affects severely the properties of soil and the quality of the groundwater, we aimed for a thorough reconstruction of the land use history of the presumed rural region. We found that extensive forest use has been the dominant land use in all time periods with even no deforestation during the medieval ages (Otto, 2000). Mode of forest operation shifted from random selection of wood via coppice use (since the 15th century) and planter forestry (since the 20th

15 century) to unmanaged woodland with the foundation of the Hainich National Park (www.nationalpark-hainich.de) in December 1997 (Otto, 2000; Röhling and Safar, 2004). Parts of the Hainich National Park, which are now unmanaged grassland/scrubland areas, had been formerly used as a military training area since 1964, particularly for tank trainings from 1980 until 1990 (Otto, 2000; Poser, 2004). Crop and pasture agriculture of the lower Hainich hillslope had been organized by agricultural production cooperatives in the former GDR time (from 1945 to 1990) and are now (since 1990) managed by

20 privately owned farmer's cooperatives.

3.3 Soil series and surface geology

The landscape of the Hainich low mountain range has been developed within the Triassic formations of the Upper Muschelkalk and Lower Keuper. As the geological strata in the study region dip NE in the direction of, but steeper than the

25 angle of surface relief, outcrops of lower/older stratigraphic units are located at the upper slope positions only. To this end, all formations outcrop in distinct zones along the eastern slope of the Hainich ridge (Fig. 2). In addition to the general NE inclination, the upper slope includes a NW-SE oriented normal fault with offsets of about 10 m. Parallel, fault bound troughs are also found near this fault. Near-surface karstification is observed for limestones outcropping at the upper hillslope. The Triassic rocks are covered by young loess loam in sheltered, concave depressions of the east-exposed slopes. Alluvial soils

30 and colluvium fill the valley bottoms. Both sediments are absent at the upper slope and increase in both thickness (max. 3.5 m) and areal cover from the middle to the lower slope.

Soils cover the entire landscape with major soil series developed from carbonate rocks ("carbonate soil series"; Rendzic Leptosols to Chromic Cambisols), siliceous rocks ("siliceous soil series"; Luvisols, Stagnosols) or alluvial sediments (WRB and German soil groups: Table 1). Cambisols are found at the upper and middle slope, Luvisols at the middle and lower

35 slope (both of them mostly used as cropland/pasture) and Stagnosols are restricted to the lower slope. Chromic Cambisols are found in local depressions and old sinkholes. Typical two layer soil profiles, developed from two different substrates, are (I) Luvisols developed from loess loam overlying (II) Chromic Cambisols developed from marlstones (Fier, 2012) (Fig. 2 and Table 1).

40 3.4 Lithology, host rock mineralogy and lithostratigraphic framework

The succession of the strata outcropping within the study area comprises Middle Triassic sedimentary rocks of the Middle and Upper Muschelkalk subgroup as well as the Lower Keuper subgroup. According to the German stratigraphy, the Middle Muschelkalk is separated into the Karlstadt, Heilbronn, and Diemel formations, the Upper Muschelkalk comprises the



Trochitenkalk, Meissner, and Warburg formations and the Lower Keuper is synonymously used for the Erfurt formation (Deutsche Stratigraphische Kommission, 2002). The Upper Muschelkalk subgroup, which hosts the target aquifers of the Hainich CZE, is organized by bio- and lithostratigraphic marker beds (Ockert and Rein 2000; Kostic and Aigner, 2004). The Triassic strata is bounded by an erosional unconformity on top, which is overlain by aeolian loess loam developed from loess deposits of the last glacial period (Weichsel glacial in Germany; Greitzke and Fiedler, 1996) and alluvial/colluvial sediments of Holocene age (Rau and Unger, 1997).

The Diemel formation (mmDO) comprises thin (1-3 cm) yellowish dolomitic marlstones, fine crystalline dolomite and rarely cavernous dolomites without any fossils, gypsum or salt. The 7 m thick Trochitenkalk formation (moTK) with thick (5-30 cm), gray, coarse bioclastic limestones (mainly rudstones with the rock forming fossil *Encrinurus liliformis*) forms a karst-fracture aquifer classifiable as intrastratal karst (Ford and Williams, 2007). Large scale (meter-scale) and consistent fractures, a high fracture index and dissolution-enlarged fractures and vugs (cf Lucia, 1983), as well as karst breccia and conduits at the base of the formation are common features. All fractures and pores are stained with red brownish (Munsell 10R6/6) coatings. Karst features in the Trochitenkalk formation occur from near surface to 90 m depth. Rock mineralogy is dominated by calcite and very low contents of dolomite with traces of quartz, muscovite, chlorite and feldspar. Based on a consistent (moTK) formation thickness, bed thickness and limestone types (Dunham, 1962) in all wells, lateral facies changes within the Trochitenkalk formation are negligible.

The 34.6 m thick Meissner formation (moM) consists of 5 m thick basal marlstones with three discrete bioclastic limestone beds (Kalkbank $\alpha/\beta/\gamma$), overlain by 29 m of alternating thin (2-5 cm) limestones (mudstones to grainstones) and marlstones. These are covered by a thick (> 60 cm) bioclastic, regional biostratigraphic marker horizon, the Cycloidesbank, which is a known regional aquifer (Grumbt et al. 1997; Hecht, 2003) of minor importance. Limestones in the Meissner formation are fracture aquifers and the mineralogical compositions are predominantly calcite and subordinate dolomite and traces of quartz, illite and feldspar. The overlying 16 m thick Warburg formation (moW) with predominantly marlstones (mineralogically: calcite, dolomite, quartz) and the 35 m thick Erfurt formation (kuE) with dolomite rocks (dolomite, calcite and quartz), siltstones, silty sandstones and claystones (illite, muscovite, chlorite and gypsum), are both unfractured aquitards (Hoppe, 1952; Hecht, 2003) and form the low permeable top-seal strata of the Upper Muschelkalk aquifer assemblages at the lower slope positions.

3.5 Aquifer stratigraphy and hydrostratigraphic standard section

In the Upper Muschelkalk strata, that represent the target formation of this study, the alternating limestone and marlstone beds create numerous aquifer and aquitard layers. Of these, the Trochitenkalk formation (moTK; referred to as HTL = Hainich transect lower aquifer assemblage by Küsel et al., 2016) is the most productive regional aquifer assemblage in current use (Hecht, 2003). It is of karst-fracture type without prominent marlstone interlayers and is sealed at the base by impermeable dolomitic marlstones of the Diemel Formation (mmDO). We observed an intact and unweathered base seal in all wells that were drilled to the base of the moTK. The second major aquifer assemblage is the Meissner formation (moM; referred to by Küsel et al. (2016) as HTU = Hainich transect upper aquifer assemblage), that contains limestone-fracture aquifers which are interbedded with marlstone-aquitards on the decimeter to meter scale (Table 2).

According to published examples for multi-storey subsurface architecture (Haag and Kaupenjohann, 2001; Heinz and Aigner, 2003; Klimchouk, 2005; Sharp, 2007), we use the term "aquifer storey" to emphasize our conceptualization of the fine-stratified setting by arbitrary definition of intervals that are dominated by fractured limestone beds and confined at the top and base by present, unfractured or low permeable beds, the latter with a minimum thickness of 80 cm.

Based on the lithological core description, the lower aquifer assemblage (HTL) represents one aquifer storey termed moTK-1, and the upper assemblage (HTU) is organized into nine aquifer storeys (moM-1 to moM-9; Table 2), sandwiched



between less permeable units. The correlation of sedimentological core logs and geophysical borehole logs infers, that the subsurface is stratified and all aquifers and aquitards are presumably continuous on the scale of the research transect (5.4 km). In the case of all aquifer storeys flow conditions are confined, preferential groundwater recharge takes place in the upper slope positions (outcrop zones) and regional discharge is towards the NE, due to lithology and orientation of the strata.

5 Due to their different lithological and bedding properties, the two aquifer assemblages HTL and HTU show significantly different aquifer characteristics: The HTL-assemblage, characterized by thick limestone packages without considerable aquitard interlayers, tends to have strong karstification features, broad fractures as well as shallow soils in the recharge area. By contrast, the HTU assemblage with its finely alternating aquifer-aquitard stratification exhibits a lesser intensity of karstification, fine fissures as flow paths and it recharges in mid slope areas with thicker soils that partially inhibit rain water

10 infiltration at lower slope areas. In the lower slope both aquifer assemblages are overlain by low to impermeable cap rocks of the Warburg formation (Upper Muschelkalk) and the Erfurt formation (Lower Keuper).

3.6 Groundwater chemistry

The groundwater in the carbonate rock landscape is classified as little to strongly mineralized earthalkaline, bicarbonatic type (site H1/2/3/4), and earthalkaline, bicarbonatic-sulfatic type (groundwater of the deep well H51 (HTL; Thüringer Landesanstalt für Umwelt, 1996). The order of abundance for dissolved ions is: $\text{Ca}^{2+} > \text{Mg}^{2+} > \text{Na}^+ > \text{K}^+$ and $\text{HCO}_3^- > \text{SO}_4^{2-} > \text{Cl}^-$ (Fig. 3). According to the groundwater subtypes of Kralik et al. (2005) the moM (HTU) waters (except for well H14) plot in the “dolomite”-field, moTK-1 (HTL)-waters (wells H13/21) and water from H14 (moM, HTU) plot in the “calcite”-field. All other moTK-1 (HTL) wells (H31/41/51) are classified as the mixed subtype (“calcite+dolomite”; Fig. 3). Two

20 contact springs in the recharge area (Hünenteich spring, Ihlefeld spring) and two karst springs in the discharge area (Kainspring, Melchiorbrunnen, coupled to NW-SE oriented fault zones: Fig. 1), are classified as carbonate-earth alkaline type, predominantly in contact with calcite in the recharge area and a calcite-dolomite mixing type in the discharge area. Hierarchical cluster analysis (HCA) reveals no multi-case clustering. Cluster 1 includes the groundwater samples from upper slope moTK-1 (HTL) wells (H13/21) and the moM well H14 (HTU). Cluster 2 encompasses the groundwater samples from

25 moTK-1 wells H31/41 (HTL) as well as from moM well H32 (HTU). Groundwater samples from moTK-1 (HTL) well H51 plot in cluster 3. Cluster 4 includes (HTU) wells H42/43/44, while cluster 5 consists of two moM (HTU) wells of the same site (H52/53; Fig. 4).

As a result of the principal component analysis (PCA) using the complete parameter set (Fig. 4a), and the parameter set without redox sensitive parameters (Fig. 4b), data points fall into very similar groupings compared to the HCA. According to

30 the PCA of the complete parameter set, the first two components (PC1 plus PC2) explain 54.9 %, and according to the parameter set without redox sensitive parameters PC1 plus PC2 explain 62.1 % of the total variability, respectively. For both PCA, the controlling factors for hydrochemical grouping are Si^{4+} , K^+ , Na^+ , HCO_3^- , Mg^{2+} for PC1 and Sr^{2+} , SO_4^{2-} , EC-25 and Cl^- for PC2.

In general, average chemical values of all aquifer storeys infer, that groundwater of the moTK-1 (HTL) aquifer exhibits

35 generally higher O_2 , SO_4^{2-} , Sr^{2+} and lower Mg^{2+} , HCO_3^- , Si^{4+} , K^+ , Na^+ and NO_3^- concentrations compared to the HTU (moM formation) aquifer assemblage when sampled at the same locations. Groundwater sampled from the moTK-1 (HTL) aquifer show consistent chemical trends from the recharge to the discharge area: ion sums increase, in particular in the concentrations of K^+ , Mg^{2+} , Si^{4+} , Sr^{2+} , SO_4^{2-} and Cl^- (Fig. 5).



4 Discussion

4.1 Groundwater recharge

Recharge areas

Preferential recharge areas for the aquifer storeys match with the outcrop zones (Fig. 2). It is reasonable to infer that catchment sizes, travel distances and residence times are generally larger for lower slope wells (site H4/5) compared to upper slope wells (site H1/2). Valley incision forces partial exfiltration of moM-3 to 9 groundwaters via contact springs and thus reduces the effective catchment size of these aquifers storeys. Additional concentrated infiltration takes place in the lines of sinkholes, which can be tracked over more than four kilometers in the middle slope between transect locations H2/3 and H4. Lineaments of sinkholes likely represent fracture zones (Smart and Hobbs, 1986; Worthington, 1999; Klimchouk, 2005) and are here related to the fault-related penetration of surface water and the subsequent subsidence of Middle Muschelkalk evaporites like salt and gypsum (Mempel, 1939; Malcher, 2014).

Soil distribution and soil development

Soil groups reflect geology and slope position: in the upper slope position and on steep slopes, the soil groups (Rendzic Leptosols, Calcaric Regosols and Chromic Cambisols) are determined by the carbonate-rock parent material (Greitzke and Fiedler, 1996; Brandtner, 1997; Rau and Unger, 1997). Chromic Cambisols are relict soils in Germany (AG Boden, 2005) and represent the final stage of decarbonatization (Rau and Unger, 1997). Soil groups in moderately inclined mid slope and toe slope positions are Luvisols and Stagnosols developed from (solifluction) mixed carbonate (marlstone) and siliceous (loess) material (Kleber, 1991; Bullmann, 2010) by continued clay relocation to the subsoil (Rau and Unger, 1997).

Infiltration properties of soils and the unsaturated zone

The thickness, clay content and clay distribution in soils influence the infiltration (Smart and Hobbs, 1986). Overall infiltration properties decrease from the upper slope towards the lower slope with increasing thickness of young cover strata like loess loam (Kleber, 1991; Bullmann, 2010). Infiltration is assumed to be inhibited by thick argillaceous soils in alluvial valleys, uvala-like depressions and local toe slope settings, with accumulations of alluvial/colluvial clay (Fig. 2). However, plateau positions (with reduced erosion) at the crest of the Hainich hillslope also show thicker cover strata and thus low infiltration. Fracture and karstification zones like sinkholes or dry valleys (in upper slope positions of the study area) promote the preferential infiltration (Smart and Hobbs, 1986; Suschka, 2007). Rendzic Leptosols of upper slope positions offer better infiltration properties (Hiekel, 2004) than Cambisols, Lithic Udorthents and argillaceous Chromic Cambisols (Brandtner, 1997). Young/initial Luvisols, developed from predominantly silty loess loam show better infiltration properties than mature Luvisols and Stagnosols with layers of subsoil clay. Two layer soil profiles (Cambisols/Luvisols overlying Chromic Cambisols) inhibit infiltration and promote soil water interflow within the topsoil or at the topsoil-subsoil interface. Water of short and heavy rain events preferentially infiltrates through macropores (desiccation cracks and biopores/earthworm burrows), bypassing the soil matrix pores (Luxmoore, 1991; Edwards and Bohlen, 1996). Intense surface karstification and fracturing is found in valleys, which represent zones of local geostructural weakness (Klimchouk, 2005) as well as the more regional fracturing found in the upper slope (Mempel, 1939; Hoppe and Seidel, 1974; Jordan and Weder, 1995).

The land use type also influences the infiltration properties (Hohnvehlmann, 1995), as it is discussed and classified by Dunne and Leopold (1978) for the United States. The soils of the former military (tank) training area very likely inhibit infiltration and favor surface runoff due to compaction. Cropland cultivation modifies soil fabrics, reduces the humic content and increases the soil bulk density. Aquifers in (fertilized) agriculturally used catchment areas (for instance aquifer moM-9), are anoxic, probably due to microbial oxygen depletion resulting from the degradation of organic carbon compounds or oxidation of inorganic electron donors. Catchment areas (defined for all individual aquifers) show a predominance of forest



land use (44.5 to 96.5 % forest). However we detected potentially agriculture related substances (NO_3^- , K^+ , Cl^-) in the wells drilled to all HTU and HTL-aquifer assemblages in middle and lower slope locations (H3/4/5) wells. This points to a significant influence of surface waters entering the aquifers vertically via fractures or sinkholes.

5 4.2 Flow path continuity and aquifer grouping inferred from geology and hydrochemistry

Although we identify two major aquifer assemblages, the chemistry of the groundwaters fall into five distinct clusters. The lithologically defined aquifer-aquitard succession in combination with the increase in karstification towards the base, and the preferential presence of groundwater at the base of limestone packages point to confined aquifers with stratigraphic flow control (Klimchouk and Ford, 2000; Goldscheider and Drew, 2007). Furthermore, hydraulic heads and chemical groundwater compositions of different aquifers at the same sites [H13/14 (cluster 1); H41/42 (cluster 2 and 4); H51/53 (cluster 3 and 5)] are significantly distinct, indicating no vertical connection. Thus we interpret the thin aquifer beds as confined, “sandwich flow type” aquifers (term: White, 1969; Klimchouk, 2005) which are interbedded with confining aquitards. The assumed lateral continuity of aquifers and aquitards results in a “layer-cake” aquifer architecture which has been demonstrated for the Upper Muschelkalk of Central Europe (Aigner, 1982, 1985; Merz, 1987; Simon, 1997; Borkhataria et al. 2005).

Secondary mineralizations, that indicate groundwater flow (for instance Liesegang banding), occur on limestone fractures. Fracturing of aquifer rocks increases close to the (NE-SW-striking) fault zones (Hoppe, 1962) and karstification follows the network of faults (Goldscheider and Drew, 2007). Red and brown iron and manganese oxides on upper to middle slope fractures (H1/2/3; cluster 1 and 2) signal temporarily unsaturated conditions, whereas green/gray fracture minerals in the lower slope domains (HTU, H4/H5, cluster 4/5) point to permanently saturated conditions (and likely anoxic conditions, for instance no oxidized Fe/Mn-minerals). Corrosion occurs as intrastatal karstification, which means one or more layers of soluble strata is covered or sandwiched between insoluble beds (Palmer, 1995). Karstification is consistently high in the thick bedded aquifer storey (moTK-1, HTL) and less pronounced in thinly bedded aquifer storeys (moM-1/4/5/6; HTU; Fig. 6) as the bed thickness controls continuity, spacing and width of joints (Goldscheider & Drew, 2007).

Principal component analysis (PCA) using the complete parameter set (a) does not simply reflect aquifer stratigraphy, as each aquifer assemblage contains more than one type of groundwater chemistry (Fig. 6). By contrast, the PCA (b) carried out with the limited parameter set (without redox-related parameters) shows a clear separation of HTL and HTU aquifer assemblages (except cluster 2). The comparison of groundwater samples, that fall in the individual clusters, with the control factors derived from the PCA (using parameter set a), depends on aquifer rock type, slope position, land use and soil group in the recharge area as well as with the proximity to karstification zones results in the following interpretation of the clusters:

Cluster 1 (upper slope HTL wells H13/21 and HTU well H14) comprises the moTK-1 aquifer storey in shallow (near surface) positions with recharge areas, exclusively used as forest. Relatively high HCO_3^- and Ca^{2+} as well as low Mg^{2+} , SO_4^{2-} , Na^+ , K^+ , Si^{4+} concentrations (Fig. 7) correspond with the pure calcite limestone (CaCO_3) aquifer lithology without any gypsum and very thin marlstone (clay mineral) interlayers.

Cluster 2 (HTL in middle slope wells H31/41 and HTU well H32) includes aquifer storeys in shallow and moderate depth with mixed forest and agricultural catchment. The sites H3/4 are located in the discharge of a prominent karstification zone with sinkholes crossing the line of the research well transect. In addition, round and elongated areas on cropland (recognized on aerial images) with increased soil thickness (inferred from soil mapping), point to former/filled sinkholes. Oxygenated groundwaters in both aquifer assemblages (thus with low Fe/Mn mobility; Hem, 1985) and a high degree in rock fracturing and fracture mineralization with Fe-/Mn-oxide minerals (HTU aquifer storeys moM-9/8/7 and 6), point to a vertical penetration with near surface groundwater via fracture zones through the HTU and in the HTL aquifers. Enhanced concentrations in Na^+ , K^+ , NO_3^- , Cl^- and TOC (Fig. 7) are likely related to agriculture and fertilizing (Matthess, 1994;



Kunkel et al, 2004). As nitrate, which is generally derived from agricultural fertilizers (Agrawal et al., 1999; Jeong, 2001), is still present in the deep aquifer waters of site H3, vertical bypassing must be faster than the denitrification process or (alternatively) descending, fault-related waters completely bypass the upper aquifers via large master joints (term: Dreybrodt, 1988; Ford and Williams, 2007), cutting through the complete overlying strata. Vertical fault-related infiltration is likely, as the hydrochemical composition does not match with the forest covered catchment of the HTL (moTK-1) aquifer storey.

Cluster 3 (HTL in footslope well H51) encompasses the moTK-1 aquifer storey in depths of greater than 85 meters, with more distant (4-5 km) forest catchment. Very high concentrations of Ca^{2+} , SO_4^{2-} , Sr^{2+} , Cl^- (and $\text{SO}_4^{2-}/\text{HCO}_3^-$ -ratios) that do not reflect the pure limestone (CaCO_3) lithology of this aquifer storey, as well as the combination with low K^+ , Na^+ , NO_3^- concentrations point to a non-surface related source of sulfatic waters. A non-agricultural source of SO_4^{2-} is supported by significantly lower sulfate concentration in the more surface-near wells of (H52/53) of the same site. Increased Cl^- concentrations could be due to dissolution of evaporites (Edmunds and Smedley, 2000). The geostructural position in the discharge of a karstification lineament (fracture zone) and the stratigraphic position (of HTL), directly overlying the Middle Muschelkalk subgroup (containing Ca-(Sr)-sulfate rocks; Jordan and Weder, 1995) point to the import of rising sulfatic Middle Muschelkalk groundwaters (Garleb, 2002; Völker and Völker, 2002). Mixing of Ca-sulfate and Ca-carbonate waters results in an oversaturation and precipitation of calcite and a decrease in alkalinity (Moral et al., 2008), which is supported by a slightly lower pH in well H51. The ascent of confined groundwaters from stratigraphically lower to higher formations, which is well known for artesian settings (Klimchouk, 2005), is assumed to be coupled to a certain threshold value of confinement and hydrostatic pressure, that is probably reached between the well sites H4/5 (cross section in Fig. 8). Alternatively, the ascent of Middle Muschelkalk groundwaters could be promoted by the lateral permeability decrease from the recharge to the discharge area within the Middle Muschelkalk aquifers of the Hainich region. This decrease in permeability is related to a “subrosion front” (probably between site H4/5; Fig. 8), as the dissolution of sulfate rocks is completed (high permeability) in the recharge area whereas impermeable sulfate rocks are still present in the discharge area (Hoppe and Seidel, 1974; Garleb, 2002).

Cluster 4 (HTU in valley-position wells H42/43/44) includes aquifer storeys in shallow depth with thick (> 5 m) alluvial (argillaceous) cover sediment in valley position, with mixed forest/agriculture/village catchment. The aquifer lithology (limestones) is reflected by high HCO_3^- groundwater concentrations. Low K^+ , Na^+ , Si^{4+} point to a small influence from marlstones (clay minerals; Bakalowicz, 1994), and thus the alluvial, argillaceous sealing strata at the top is very likely intact. High $\text{Fe}^{(2+ \text{ and } 3+)}$, $\text{Mn}^{(2+ \text{ and } 4+)}$ and low SO_4^{2-} concentrations correspond to a low redox potential and the absence of dissolved oxygen, controlling the mobility of these ions (Hem, 1985; Hsu et al., 2010). Under the given physico-chemical conditions, the NO_3^- concentration is low due to the denitrification by anaerobic bacteria (Agrawal et al., 1999).

Cluster 5 (HTU in footslope wells H52, H53) comprises aquifer storeys covered by very thick (> 40 m), low permeable cover strata (Erfurt formation, Warburg formation) and long (flow) distances (> 3 km) to their recharge area. Based on the aquifer lithology, groundwater discharges through interbedded limestones and marlstones. High K^+ , Na^+ and Mg^{2+} concentrations point to long residence times with clay minerals (Bakalowicz, 1994). High silica concentrations are proportional to (long) residence times of groundwater in the subsurface (Khan and Umar, 2010). Low NO_3^- concentrations correspond with low redox potentials due to the denitrification of nitrate (Jang and Liu, 2005).

All in all, hierarchical clusters can reflect differences in the length of the flow path (residence time), and therefore differential amounts of rock-water and microbial interaction, the land use type (forest/agriculture) in the recharge area, and external sources of sulfate and magnesium (for instance lower slope well H51; cluster 3). To this end, the effectiveness of the basal and top sealing aquitard layers has a significant influence on the groundwater chemistry.

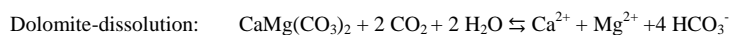
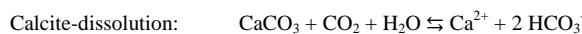
In this study we distinguish between three different modes of subsurface water flow: (1) Vertical and descending water flow



(gravitationally driven) takes place in the recharge areas of the aquifers at the crest and upper slope zones of the Hainich hillslope (including sites H1/2, HTL, cluster 1). (2) Bedding-parallel, confined groundwater flow (stratigraphic flow control, Goldscheider, 2005) occurs in the tectonically undisturbed zones, with intact aquitard interbeds, between, and downstream the two sinkhole lineaments. Confined flow could explain the long water-rock contact times in cluster 5 (HTU) and also the very low concentrations of NO_3^- , NO_2^- and NH_4^+ (with potential agricultural origin) of cluster 4 (HTU)-aquifers, which are sealed at the top. Bedding parallel flow is also supposed for fractures with small fault displacements that do not exceed the thickness of the interbedded aquitard (compare to Goldscheider & Drew, 2007). This situation is probably applied to the straight and equidistant oblique valleys, which are probably fault zones. (3) Cross-formational flow through open faults is assumed to take place in fracture zones (Worthington, 1999; Goldscheider & Drew, 2007), tracked by lineaments of sinkholes (Mempel, 1939; Hoppe, 1962; Smart and Hobbs, 1986; Jordan and Weder, 1995). Descending flow of surface waters very likely takes place in the middle slope sinkholes with the sites H3/4 downstream (cluster 2, HTL and HTU wells) and ascending groundwater flow is supposed for the lower slope well H51 (cluster 3 HTU, Fig. 8).

4.3 Controls for variations in karstification

Karstification and carbonate dissolution is mainly controlled by CO_2 exchange, and thus related to the concentration of dissolved CO_2 in the groundwater (Zötl, 1974; Powell, 1977; Dreybroth, 1981; Hoffer-French and Herman, 1989) as it is exemplified below:



The production of metabolic carbon dioxide within the soils is discussed as a major driving force for the karstification in the near surface carbonate rocks (Krämer, 1988; Ford and Williams, 2007), for instance in epikarst settings (Pan and Cao, 1999). With increasing distance from soil related CO_2 -sources, the corrosion and the width of fractures and conduits decrease (Ford and Williams, 2007; Williams, 2008). The dissolution of calcite is a relatively fast reaction (Plummer et al., 1979). Kinetic calculations of Dreybroth (1981) infer that CaCO_3 -saturation within karst groundwater in general is reached after a few meters. To this end, the hydrological system in karst groundwaters theoretically grades from wholly karstic to non-karstic (Ford and Williams, 2007) with 50-80 % of carbonate dissolution occurring in the uppermost 10 meters of the subsurface in unconfined settings (Smith and Atkinson, 1976). This contradicts the observed karst features and high CO_2 concentrations in our wells 4 to 5 kilometers away from the groundwater catchment.

One aspect for subsurface carbonate dissolution is the continued release of carbon dioxide by microbes living in the groundwater and rocks far away from the groundwater catchment (Lian et al., 2011). According to Gabrovšek et al. (2000), evenly distributed microorganisms deliver constant production rates of carbon dioxide, as long as organic matter and oxygen is available. In addition, microbes produce organic acids during fermentation under lowered oxygen concentrations that occur in a deprotonated form under pH neutral conditions (for instance acetate or propionate) or enzymes (carbonic anhydrases) that both enhance limestone weathering (Lian et al., 2011). In addition to organic acids and alcohols released during fermentation, high amounts of carbon dioxide are released. Also other anaerobic processes using Fe(III) or sulfate as terminal electron acceptor produce carbon dioxide which can be applied to the anoxic aquifer storey moM-8 (HTU, cluster 4). Alternatively, karstification may be to a large extent triggered and maintained to the provision of strongly undersaturated (mean ion sums: 123 mg/l for forest, 65 mg/l for grassland) and weakly acidic (pH: 5.9 for forest, 6.0 for grassland), precipitation-fed seepage of CO_2 -containing water via fracture zones and lines of sinkholes. Such deep penetration of surface waters is supported by the presence of agriculture-born substances in the deep aquifer storey moTK-1 (HTL) of the well sites H4/5. As the groundwater compositions of all aquifer storeys are chemically different, mixing corrosion (Bögli, 1964; Wigley and Plummer, 1976) is also possible, for instance through the cross formational mixing of HCO_3^- groundwater with



rising groundwater from the Middle Muschelkalk via fracture zones. Mixing corrosion is based on the mixing of two CO_2 - HCO_3^- waters with different chemical composition and both saturated in carbon dioxide (Palmer, 1995). However, more recent studies (Gabrovšek and Dreybrodt, 2000) show, that the dissolution kinetics of carbonate minerals strongly affect the intensity of karstification. In addition to the chemical aspects, turbulent flow in conduits, which is rather normal for karst
5 aquifers (White, 1969), could enhance pre-existing fractures and conduits mechanically (Howard and Groves, 1995).

5 Conclusions

We investigated the origin of groundwater found in aquifers of the eastern slope of the Thuringian Basin developed in carbonate rocks, with the goal of understanding the potential links between geology, topography, soils, land use, water
10 recharge and chemical evolution. Based on the mapping of the outcrops of aquifer storeys and infiltration pathways in near surface fractures and karst, we found that potential rain water infiltration times for the target aquifers are short, hydraulic conductivities are assumed to be high and the retention potential for airborne or soil-borne solutes is relatively low, but higher than for unconfined karst/settings. This results in a lower groundwater vulnerability, than recorded for unconfined karst/carbonate settings (Doerfliger et al., 1999; Witowski et al., 2002) that do not show a stratified aquifer/aquitard
15 subsurface. Due to lithological differences between HTL (moTK-1) and HTU (moM-1 to 9), the limestone-dominated, highly karstified lower aquifer assemblage (HTL) is significantly more vulnerable with regard to anthropogenic influence and pollution.

Pedological/geological data infers that soil-born particulate (for instance soil microorganisms) and dissolved substances with sizes up to tens of microns could be transported to and between the partially disjoint aquifers levels. This applies especially
20 for Rendzic Leptosols on limestones (with earthworm borrows) and for highly permeable silt-dominated Luvisols, developed from loess, that directly cover fractured limestones. The geological sandwich structure enforces confined groundwater flow conditions. Within the aquifer-aquitard-sandwich, fast conduit groundwater flow takes place in the karstified and fractured moTK-1 (HTL) and the moM-1 (HTU) aquifer storeys, whereas slow diffusion in slightly fractured, thin aquifers beds is anticipated in the moM-2 to moM-9 (HTU) aquifer storeys. This results in oxygenated moTK-1 and moM-1 groundwaters
25 and a significant oxygen consumption/deficiency (coupled to the mobility of Fe^{2+} and Mn^{2+} -ions and the low mobility of NO_3^- and SO_4^- ions) in the moM-2 to 9 waters, resulting in completely different milieu conditions for geochemical processes and supposedly also for the life in the subsurface.

Data availability

Plot data will be deposited on the BExIS2 (<http://bexis2.uni-jena.de>) data portal of the CRC AquaDiva (<https://aquadiva-pub1.inf-bb.uni-jena.de>). Access to the AquaDiva data portal for review purposes is granted.

Hydrochemical data will not be shared publically at this point of time, as this paper represents the first of a series of three related papers, using similar data sets for different aims. For instance the prepared time series analysis as well as flow and transport models will rely on the same data sets.

35

Team list

Bernd Kohlhepp (BK), Robert Lehmann (RL), Paul Seeber (PS), Kirsten Küsel (KK), Susan E. Trumbore (SET) and Kai U. Totsche (KUT).

40 Author contribution

BK, RL, PS and KUT wrote the paper in collaboration. RL and BK comprehensively organized and BK conducted the geological mapping, soil mapping, as well as the analysis and correlation of drill cores and geophysical logs. RL organized and partly conducted the groundwater and surface water monitoring and carried out main parts of the literature research and



obtained authorization from authorities and landowners/companies. PS carried out parts of the soil mapping/description and hydrochemical analyses and carried out the descriptive and multivariate statistics. SET and KK provided editorial comments on the manuscript. KUT coordinated the subproject and supervised the field work, data analysis, data presentation and manuscript preparation. KK, KUT and SET are speakers of the CRC AquaDiva.

5

Competing interests

The authors declare that the research was conducted in the absence of any commercial or financial relationships that could be construed as a potential conflict of interest.

10 Acknowledgements

The work has been (partly) funded by the Deutsche Forschungsgemeinschaft (DFG) CRC 1076 "AquaDiva" and the state of Thuringia 'ProExzellenz' initiative AquaDiv@Jena (107-1). Field work permits were issued by the responsible state environmental offices of Thuringia, local authorities and landowners. We thank Christine Hess for scientific coordination. Heiko Minkmar supported the field surveys and conducted water and ramcore samplings. Matthias Händel carried out the
15 FT-IR and XRD measurements.

References

- AG Boden: Bodenkundliche Kartieranleitung, 5. Edition, Ad-hoc-Arbeitsgruppe Boden der Geologischen Landesämter und der Bundesanstalt für Geowissenschaften und Rohstoffe der Bundesregierung Deutschland, Schweizerbart, Stuttgart,
20 Hannover, 438, 2005.
- Agrawal, G.D., Lunkad, S.K., Malkhed, T.: Diffuse agricultural nitrate pollution of groundwaters in India, *Water Sci. Technol.* 39, 67–75, 1999.
- Aigner, T.: Calcareous tempestites: storm-dominated stratification in Upper Muschelkalk limestones (Middle Triassic, SW-Germany), in: *Cyclic event stratification*, edited by: Einsele, G. and Seilacher, A., Springer, Berlin, Heidelberg, New
25 York, 190-198, 1982.
- Aigner, T.: Storm depositional systems: Dynamic stratigraphy in modern and ancient shallow-marine sequences, *Lect. Notes Earth Sci.*, 3, Springer, Berlin, Heidelberg, New York, 174, 1985.
- Allocca, V., Manna, F. and De Vita, P.: Estimating annual groundwater recharge coefficient for karst aquifers of the southern Apennines (Italy), *Hydrol. Earth Syst. Sc.*, 18, 803–817, doi:10.5194/hess-18-803-2014, 2014.
- 30 Backhaus, K., Erichson, B., Plinke, W., Weiber, R.: *Multivariate Analysemethoden: eine anwendungsorientierte Einführung*, 14, Springer, Berlin, Heidelberg, 647, 2016.
- Bakalowicz, M.: Water geochemistry: water quality and dynamics, *Groundw. Ecol.* 1, 97–127, 1994.
- Barberá, J. A. and Andreo, B.: Functioning of a karst aquifer from S Spain under highly variable climate conditions, deduced from hydrochemical records, *Environ. Earth Sci.*, 65, 2337–2349, doi:10.1007/s12665-011-1382-4, 2012.
- 35 Bögli, A.: Mischungskorrosion - Ein Beitrag zum Verkarstungsproblem, *Erdkunde*, 18, 83-92, doi:10.3112/erdkunde.1964.02.0, 1964.
- Borkhataria, R., Aigner, T., Poeppelreiter, M. C., Pipping, J. C. P.: Characterization of epeiric "layer-cake" carbonate reservoirs: Upper Muschelkalk (Middle Triassic), The Netherlands, *J. Petrol. Geol.*, 28(2), 15-42, doi:10.1111/j.1747-5457.2005.tb00076.x, 2005.
- 40 Brandtner, W.: Böden, in: *Erläuterungen zur Geologischen Karte 1:25000 von Thüringen, Blatt 4729 (Schlotheim) und 4730 (Ebeleben)* edited by: Grumbt, E., Kästner, H., Lützner, H., 210-216, Thüringer Landesanstalt für Umwelt und Geologie, Weimar, 1997.



- Bullmann, H.: Eigenschaften und Genese periglazialer Deckschichten des Muschelkalks in einem Teilgebiet der Ostthüringer Triaslandschaft, PhD-thesis University of Leipzig, 210, 2010.
- Canora, F., Fidelibus, M.D., Sciortino, A., Spilotro, G.: Variation of infiltration rate through karstic surfaces due to land use changes, *Eng. Geol.*, 99, 210-227, doi:10.1016/j.enggeo.2007.11.018, 2008.
- 5 Cattell, R. B.: The scree test for the number of factors, *Multivar. Behav. Res.*, 1, 245–276, doi:10.1207/s15327906mbr0102_10, 1966.
- Dafny, E., Burg, A., Gvirtzman, H.: Effects of Karst and geological structure on groundwater flow: The case of Yarqon-Taninim Aquifer, Israel, *J. Hydrol.*, 389(3), 260-275, doi:10.1016/j.jhydrol.2010.05.038, 2010.
- Deutsche Stratigraphische Kommission (2002): Stratigraphische Tabelle von Deutschland (STD 2002), 1. Edition, Stein, 10 Potsdam.
- Dibbern, D., Schmalwasser, A., Lüders, T., Totsche, K. U.: Selective transport of plant root-associated bacterial populations in agricultural soils upon snowmelt, *Soil Biol. Biochem.*, 69, 187-196, 2014.
- DIN EN ISO 14689-1: Geotechnical investigation and testing – Identification and classification of rock –Part 1: Identification and description (ISO 14689-1:2003), 26, 2013.
- 15 Doerfliger, N., Jeannin, P.Y., Zwahlen, F.: Water vulnerability assessment in karst environments: a new method of defining protection areas using a multi-attribute approach and GIS tools (EPIK method), *Environ. Geol.*, 39(2), 165-176, 1999.
- Dreybroth, W.: Mixing corrosion in CaCO₃-CO₂-H₂O-Systems and its role in the karstification of limestone areas, *Chem. Geol.*, 32, 221-236., doi:10.1016/0009-2541(81)90145-5, 1981.
- Dreybroth, W.: Processes in karst systems – physics, chemistry and geology, Springer, Heidelberg, New York, 288, 1988.
- 20 Dunham, R. J.: Classification of carbonate rocks according to depositional texture, in: Classification of carbonate rocks, edited by: Ham, W. E., AAPG Memoir, 1, 108–121, 1962.
- Dunne, T. and Leopold, L.B.: Water in environmental planning. Freeman: New York, 818 p. 1978.
- Edmunds, W.M. and Smedley, P.L.: Residence time indicators in groundwater: the East Midlands Triassic sandstone aquifer, *Appl. Geochem.*, 15, 737-752, 2000.
- 25 Edwards C. A. and Bohlen P. J.: The biology and ecology of earthworms. Chapman and Hall, London, 426, 1996.
- Fier, A.: Entstehung, Eigenschaften und Klassifikation tonreicher Unterbodenhorizonte auf Carbonatgesteinen in norddeutschen Berg- und Hügelländern, PhD-thesis, University of Halle, 190, 2012.
- Ford, D. C. and Williams, P.W.: Karst Hydrogeology and Geomorphology, Wiley: Chichester, 561, 2007.
- Furtak, H. and Langguth, H. R.: Zur hydrochemischen Kennzeichnung von Grundwässern und Grundwassertypen mittels 30 Kennzahlen, Mem. IAH-Congress, Hannover, 86-96, 1967.
- Gabrovšek, F. and Dreybrodt, W.: Role of mixing corrosion in calcite-aggressive H₂O-CO₂-CaCO₃ solutions in the early evolution of karst aquifers in limestone, *Water Resour. Res.*, 36, 1179-1188, doi:10.1029/1999WR900337, 2000.
- Gabrovšek, F., Menne, B., Dreybrodt, Q.: A model for early evolution of karst conduits affected by subterranean CO₂ sources, *Environ. Geol.*, 39(6), 531-543, doi:10.1007/s002540050464, 2000.
- 35 Garleb, H.: Zu einigen hydrogeochemischen Problemen bei der Erkundung von Grundwasser in der Trias des Thüringer Beckens, *Mitteilungsblatt des Thüringischen Geologischen Vereins*, 15, 41-45, 2002.
- Gleixner, G.: Soil organic matter dynamics: a biological perspective derived from the use of compound-specific isotopes studies, *Ecol. Res.*, 28, 683-695. doi:10.1007/s11284-012-1022-9, 2013.
- Goldscheider, N.: Fold structure and underground drainage pattern in the alpine karst system Hochfien-Gottesacker, *Eclogae 40 Geol. Helv.*, 98, 1-17, 2005.
- Goldscheider, N. and Drew, D.: Methods in Karst Hydrogeology, International Contributions to Hydrogeology, 26, Taylor & Francis, Lodon, Leiden, New York, Philadelphia, Singapore, 264, 2007.
- Gradstein, F. M., Ogg, J. G., Smith, A. G. (2004): A Geologic Time Scale, 1, Cambridge University Press: Cambridge.



- Greitzke, A. and Fiedler, H. J.: Schuttdecken und Bodentypen entlang einer Catena auf Muschelkalk in Buchenbeständen des Hainich (Nordwest-Thüringen), *Archiv für Naturschutz und Landschaftsforschung*, 34, 257-268, 1996.
- Grumbt, E., Kästner, H., Lützner, H.: Erläuterungen zur Geologischen Karte 1:25000 von Thüringen, Blatt 4729 (Schlotheim) und 4730 (Ebeleben), *Thüringer Landesanstalt für Umwelt und Geologie*, Weimar, 262, 1997.
- 5 Guggenberger, G. and Kaiser, K.: Dissolved organic matter in soil: challenging the paradigm of sorptive preservation, *Geoderma*, 113, 293-310, doi:10.1016/s0016-7061(02)00366-x, 2003.
- Haag, D. and Kaupenjohann, M.: Landscape fate of nitrate fluxes and emissions in Central Europe: A critical review of concepts, data, and models for transport and retention, *Agriculture, Ecosystems and Environment*, 86(1), 1-21, 2001.
- Hecht, G.: Grundwässer, in: *Geologie von Thüringen*, edited by Seidel, G., Schweizerbart: Stuttgart, 586-529, 2003.
- 10 Heinz, J. and Aigner, T.: Hierarchical dynamic stratigraphy in various Quaternary gravel deposits, Rhine glacier area (SW Germany): implications for hydrostratigraphy, *Int. J. Earth Sci.*, 92(6), 923-938, 2003.
- Hem, J.D.: *Study and Interpretation of the chemical characteristics of natural water*, third edition, U.S. Geological Survey, Water Supply Paper 2254, U.S. Geological Survey, Alexandria, 263, 1985.
- Hiekel, W., Fritzlar, F., Nöllert, A., and Westhus, W.: *Die Naturräume Thüringens*, Naturschutzreport 21, Thüringer Landesanstalt für Umwelt und Geologie, Jena, 364, 2004.
- 15 Hoffer-French, K. J. and Herman, J.S.: Evaluation of hydrological and biological influences on CO₂ fluxes from a karst stream, *J. Hydrol.*, 108, 189-212, doi:10.1016/0022-1694(89)90283-7, 1989.
- Hohnvehlmann, K.: Böden, in: *Erläuterungen zur Geologischen Karte von Thüringen, Blatt 4731 (Greussen)*, edited by: Unger, K. P., Cebulla, R., Hohnvehlmann, K., Holzhey, G., Kuhn, G., Meissner, M., Pustal, I., Schröder, N., Seidel, G., Thüringer Landesanstalt für Umwelt und Geologie, Weimar, 150, 1995.
- 20 Hoppe, W.: *Die hydrogeologischen Grundlagen der Wasserversorgung in Thüringen*, Fischer, Jena, 109, 1952.
- Hoppe, W.: Die Bedeutung der herzynischen Störungszonen für die Grundwasserführung des Thüringer Beckens, *Geologie*, 11, 679-699, 1962.
- Hoppe, W. and Seidel, G.: *Geologie von Thüringen*, Haack, Gotha, 1000p. 1974.
- 25 Howard, A. D. and Groves, C. G.: Early development of karst systems, *Water Resour. Res.*, 31(1), 19-26, 1995.
- Hsu, C.-H., Han, S.-T., Kao, Y.-H., Liu, C.-W.: Redox characteristics and zonation of arsenic-affected multi-layers aquifers in the Choushui River alluvial fan, Taiwan, *J. Hydrol.*, 391, 351-366, 2010.
- IUSS Working Group WRB: *World reference base for soil resources (WRB)*, World soil resources reports, FAO, Rom, 103, 2006.
- 30 Jang, C.S. and Liu, C.W.: Contamination potential of nitrogen compounds in the heterogeneous aquifers of the Choushui River alluvial fan, Taiwan, *Journal of Contaminant Hydrology*, 79, 135-155, 2005.
- Jeong, C.H.: Effect of land use and urbanization on hydrochemistry and contamination of groundwater from Taejon area, Korea, *J. Hydrol.*, 253, 194-210, 2001.
- Jordan, H. and Weder, H. J.: *Hydrogeologie und Methoden*, Regionale Hydrogeologie: Mecklenburg-Vorpommern, Brandenburg und Berlin, Sachsen-Anhalt, Sachsen, Thüringen, Enke, Stuttgart, 601, 1995.
- 35 Kaiser, E.: *Erläuterungen zur geologischen Karte von Preussen und benachbarten Bundesstaaten, Blatt 4828 (Langula)*, Königlich Preussische Geologische Landesanstalt und Bergakademie: Berlin, 58, 1905.
- Khan, M.M.A. and Umar, R.: Significance of silica analysis in groundwater in parts of Central Ganga Plain, Uttar Pradesh, India, *Curr. Sci.*, 98(9), 1237-1240, 2010.
- 40 Kleber, A.: Gliederung und Eigenschaften der Hang-Schuttdecken und ihre Bedeutung für die Bodengeneese, *Mitteilungen der deutschen bodenkundlichen Gesellschaft*, 66(2), 807-809, 1991.
- Kley, J. and Voigt, T.: Late Cretaceous intraplate thrusting in central Europe: Effect of Africa-Iberia-Europe convergence, not Alpine collision, *Geology* 36(11), 839-842, doi:10.1130/G24930A.1, 2008.



- Klimchouk, A.: Conceptualisation of speleogenesis in multi-storey artesian systems: a model of transverse speleogenesis, *Int. J. Speleol.*, 34(1-2), 45-64, doi:10.5038/1827-806X.34.1.4, 2005.
- Klimchouk, A. B. and Ford, D. C.: Types of Karst and Evolution of Hydrogeologic Setting, in: *Speleogenesis - Evolution of karst aquifers*, edited by: Klimchouk, A. B., Ford, D. C., Palmer, A.N. and Dreybrodt, W., Huntsville, AL: National Speleological Society of America, 45-53, 2000.
- 5 Köhler, K., Duijnsveld, W., H.M., and Böttcher, J.: Nitrogen fertilization and nitrate leaching into groundwater on arable sandy soils, *J. Plant Nutr. Soil Sci.*, 169, 185-195, doi:10.1002/jpln.200521765, 2006.
- König, E.: *Das Hainichgebiet und seine Karsterscheinungen*, Thüringer Höhlen, 4, 92-101, 1930.
- Kostic, B. and Aigner, T.: Sedimentary and poroperm anatomy of shoal-water carbonates (Muschelkalk, South-German Basin): an outcrop-analogue study of inter-well spacing scale, *Facies*, 50, 113-131, doi:10.1007/s10347-004-0003-z, 10 2004.
- Kottek, M. J., Grieser, C., Beck, B., Rudolf, F., Rubel, F.: World map of the Koeppen-Geiger climate classification updated, *Meteorol. Z.*, 15, 259-263, doi:10.1127/0941-2948/2006/0130, 2006.
- Kraemer, S.: Groundwater flow pattern in joint-controlled networks and cave development, *Proc. Second Conference on Environmental Problems in Karst Terranes and Their Solutions*, Nashville, November 1988, 17-27, 1988.
- 15 Kralik, M., Zieritz, I., Grath, J., Vincze, G., Philippitsch, R. and Pavlik, H.: *Hydrochemische Karte Österreichs: Oberflächennaher Grundwasserkörper und Fließgewässer, Mittelwerte von Wassererhebungsdaten (WGEV-Daten) 1991-2001*, Berichte BE-269, 2. Revised edition, Vienna, 14, 2005.
- Kunkel, R., Voigt, H.-J., Wendland, F., Hannappel, S.: Die natürliche, ubiquitär überprägte Grundwasserbeschaffenheit in Deutschland, *Schriften des Forschungszentrums Jülich, Reihe Umwelt/Environment*, 47, Forschungszentrum Jülich, Jülich, 204, 2004.
- 20 Küsel, K., Totsche, K.U., Trumbore, S. E., Lehmann, R., Steinhäuser, C. and Herrmann M.: How Deep Can Surface Signals Be Traced in the Critical Zone? Merging Biodiversity with Biogeochemistry Research in a Central German Muschelkalk Landscape, *Front. Earth Sci.*, 32(4), 1-18, doi:10.3389/feart.2016.00032, 2016.
- 25 Lian B., Yuan D.X., Liu Z. H.: Effect of microbes on karstification in karst ecosystems, *Chinese Science Bulletin*, 56, 3743-3747, doi:10.1007/s11434-011-4648-z, 2011.
- Lucia, F. J.: Petrophysical parameters estimated from visual descriptions of carbonate rocks: A field classification of carbonate pore space, *J. Petrol. Technol.*, 216, 221-224, doi:10.2118/10073-PA, 1983.
- Luxmoore R. J.: On preferential flow and its measurement, in: Gish, T.J., Shirmohammadi, A. (Eds.): *Preferential flow: proceedings of the national symposium*. Am. Soc. Agric. Eng., St Joseph, MI, 113-121, 1991.
- 30 Malcher, G.: *Karstland Thüringen - Morphologie Hydrologie in Thüringen*, in: *Thüringen - Karst und Höhle 2011-2014*, Verband der Deutschen Höhlen und Karstforscher, München, 9-24, 2014.
- Matthess, G.: *Lehrbuch der Hydrogeologie, Band 2, Die Beschaffenheit des Grundwassers*, Bornträger, Berlin, Stuttgart, 483, 1994.
- 35 Mempel, G.: Die hydrogeologischen Verhältnisse von Nordwest-Thüringen, *Jahrbuch der Preußischen Geologischen Landesanstalt*, 59, Preußische Geologische Landesanstalt, Berlin, 587-646, 1939.
- Merz, G.: Zur Petrographie, Stratigraphie, Paläogeographie und Hydrogeologie des Muschelkalks (Trias) im Thüringer Becken, *Zeitschrift der geologischen Wissenschaften*, 15(4), 457-473, 1987.
- Moral, F., Cruz-Sanjulián, J.J., Olías, M.: Geochemical evolution of groundwater in the carbonate aquifers of Sierra de Segura (Betic Cordillera, southern Spain), *J. Hydrol.*, 281-296, 2008.
- 40 Moore, P. J., Martin, J. B., Sreaton, E. J.: Geochemical and statistical evidence of recharge, mixing, and controls on spring discharge in an eogenetic karst aquifer, *J. Hydrol.*, 376, 443-455, doi:10.1016/j.jhydrol.2009.07.052, 2009.



- Müller, K., Deurer, M., Hartmann, H., Bach, M., Spiteller, M., and Frede, H.: Hydrological characterisation of pesticide loads applying hydrograph separation at different scales in a German catchment., *J. Hydrol.* 273, 1-17, doi:10.1016/S0022-1694(02)00315-3, 2003.
- Münch, J. M., Totsche, K.U. and Kaiser, K.: Physicochemical factors controlling the release of dissolved organic dissolved organic carbon release in forest subsoils - a column study. *Eur. J. Soil Sci.*, 53, 311-320, doi:10.1046/j.1365-2389.2002.00439.x, 2002.
- Nennstiel, K.: Springquellen und andere starke Quellen Thüringens, *Beiträge zur Geologie von Thüringen*, 3, 33-66., 1933.
- Ockert, W. and Rein, S.: Biostratigraphische Gliederung des Oberen Muschelkalkes von Thüringen, *Beiträge zur Geologie von Thüringen*, 7, 195-228, 2000.
- Otto, C.: Historische Landschaftsanalyse im Nationalpark Hainich und deren Möglichkeiten der Anwendung, diploma thesis, Fachhochschule Eberswalde, 87, 2000.
- Palmer A. N.: Geochemical models for the origin of macroscopic solution porosity in carbonate rocks, in: *Unconformities and porosity in carbonate strata*, edited by: Budd A. D., Saller A. H. and Harris P.M., AAPG Memoir, 63, Tulsa (Oklahoma), 77-101, 1995.
- Pan, G. X. and Cao, J. H.: Karstification in epikarst zones: The earth surface ecosystem processes taking soil as a medium, *Carsol. Sin.*, 18, 287-296, 1999.
- Patzelt, G.: *Der Hainich*, Cordier, Heiligenstadt, 48p., 1998.
- Piper, A. M.: A graphic procedure in the geochemical interpretation of water analysis, *Trans. Amer. Geophys. Union*, 25, 914-928, doi:10.1029/TR025i006p00914, 1944.
- Plummer, L.N., Parkhurst, D.L., Wigley, T.M.L.: Critical review of kinetics of calcite dissolution and precipitation, in: *Chemical Modelling in Aqueous Systems, Speciation, Sorption, Solubility and Kinetics*, edited by: Jenne, E.A, Am. Chem. Soc. Symp. Ser., 93, 537-573, 1979.
- Poser, S.: Rekonstruktion der Nutzungsgeschichte für einen Teilbereich des NLP Hainich mit Anlage vegetationskundlicher Dauerbeobachtungsflächen und Vorschlägen zur Besucherinformation, Diploma thesis, Fachhochschule Anhalt, 108, 2004.
- Powell, R. L.: Joint pattern and solution channel evaluation in Indiana, in: *Proceedings of the 12th International Congress on Karst Hydrology*, edited by: Tolson, J.S. and Doyle F.L., Int. Assoc. Hydrogeol., Mere. 12, Huntsville Press, Huntsville, Alabama, 255-269, 1977.
- Pronk, M., Goldscheider, N., Zopfi, J., Zwahlen, F.: Percolation and Particle Transport in the Unsaturated Zone of a Karst Aquifer, *Ground Water*, 47(3), 361-369, doi:10.1111/j.1745-6584.2008.00509.x, 2009.
- Rau, D. and Unger, K. P.: Erläuterungen zur Bodenkarte von Thüringen, Blatt 4732 (Kindelbrück), Thüringer Landesanstalt für Geologie und Umwelt, Weimar, 108, 1997.
- Röhling, S. and Safar, D.: Forstgeschichte und waldbauliche Nutzung des Weberstedter Holzes ab dem 18. Jahrhundert im heutigen Nationalpark Hainich, *Belegarbeit Lehrgebiet Forstgeschichte*, University of Dresden, 24, 2004.
- Schrumpf, M. K., Kaiser, G., Guggenberger, T., Persson, I., Kögel-Knabner, E., Schulze, D.: Storage and stability of organic carbon in soils as related to depth, occlusion within aggregates and attachment to minerals, *Biogeosciences*, 10, 1675-1691, doi:10.5194/bg-10-1675-2013, 2013.
- Sharp, John M., Jr.: *A Glossary of Hydrogeological Terms*, Department of Geological Sciences, The University of Texas: Austin (Texas), 63, 2007.
- Simon, T.: The Muschelkalk karst in southwest Germany, in: *Tracer hydrology 97 - proceedings of the international symposium on water tracing*, edited by: Kranjc, A., Portoroz (Slovenia), 26-31 May 1997, 297-286, 1997.
- Smart, P. L. and Hobbs, S. L.: Characterization of carbonate aquifers - A conceptual base, in: *Environmental problems in karst terranes and their solutions: Bowling Green, KY*, 1-14, 1986.



- Smith, D.I. and Atkinson, T.C.: Process, landforms and climate in limestone regions, in: *Geomorphology and Climate*, edited by: Derbyshire, E., John Wiley & Sons, Chichester, 369-409, 1976.
- Steward, D. R., Yang, X., Lauwo, S. Y., Staggenborg, S. A., Macpherson, G. L., Welch, S. M.: From precipitation to groundwater baseflow in a native prairie ecosystem: a regional study of the Konza LTER in the Flint Hills of Kansas, USA, *Hydrol. Earth Syst. Sci.*, 15, 3181–3194, doi:10.5194/hess-15-3181-2011, 2011.
- 5 Suk, H. and Lee, K. K.: Characterization of a Ground Water Hydrochemical System Through Multivariate Analysis: Clustering Into Ground Water Zones, *Ground Water*, 37(3), 348-366, doi:10.1111/j.1745-6584.1999.tb01112.x, 1999.
- Suschka, A.: Erdfälle im Nationalpark Hainich (Thüringen): Natürliche und anthropogen bedingte Veränderungen von Erdfallstandorten in die Umweltbildung, diploma thesis, University of Greifswald, 96, 2007.
- 10 Thüringer Landesanstalt für Umwelt: Grundwasser in Thüringen: Bericht zu Menge und Beschaffenheit, Thüringer Landesanstalt für Umwelt und Thüringer Landesanstalt für Geologie, Erfurt, 163, 1996.
- Thüringer Landesanstalt für Umwelt und Geologie: Umwelt regional, available at: http://www.tlug-jena.de/uw_raum/umweltregional/uh/uh09.html, last access: January 2016.
- Totsche, K.U., Jann, S. and Kögel-Knabner, I.: Release of polycyclic aromatic hydrocarbons, dissolved organic carbon, and suspended matter from disturbed NAPL-contaminated gravelly soil material, *Vadose Zone J.*, 5, 469-479, doi:10.2136/vzj2005.0057, 2006.
- 15 Totsche, K.U., Jann, S. and Kögel-Knabner, I.: Single event driven release of PAH, colloids and suspended matter under natural conditions. *Vadose Zone J.*, 6, 233-243, doi:10.2136/vzj2006.0083, 2007.
- Urich, P.B.: Land use in karst terrain: review of impacts of primary activities on temperate karst ecosystems, *Department of Conservation*, Wellington, 58, 2002.
- 20 Voigt, T., von Eynatten, H. and Franzke, H. J.: Late Cretaceous unconformities in the Subhercynian Cretaceous Basin (Germany), *Acta Geol. Pol.*, 54, 673-694, 2004.
- Völker, C. and Völker, R.: Bemerkenswertes zu Karstquellen im Bereich Mühlhausen und des Eichsfeldes, in: *Die Geologie von NW Thüringen*, Exkursionsführer, 10-17, 2002.
- 25 Ward, J.H.: Hierarchical Grouping to Optimize an Objective Function, *J. Am. Statist. Assoc.*, 48, 236–244, 1963.
- Wätzel, A.: Geologische Heimatkunde des Unstrut-Hainich-Kreises, *Mühlhäuser Beiträge*, 30, 20-41, 2007.
- Weigand, H. and Totsche, K. U.: Flow and reactivity effects on dissolved organic matter transport in soil columns, *Soil Sci. Soc. Am. J.*, 62, 1268-1274, doi:10.2136/sssaj1998.03615995006200050017x, 1998.
- White, W. B.: Conceptual Models for Carbonate Aquifers (reprint 2012), *Ground Water*, 7(3), 180-186, 1969.
- 30 Wigley, T. M. L. and Plummer, L. N.: Mixing of carbonate waters, *Geochim. Cosmochim. Ac.*, 40, 989, 1976.
- Williams P.W.: The role of the epikarst in karst and cave hydrogeology: a review, *International J. Speleol.*, 37, no. 1, Bologna (Italy), 1-10, doi:10.5038/1827-806X.37.1.1, 2008.
- Witkowski, A. J., Rubin, K., Kowalczyk, A., Rózkowski, A., Wrobel, J.: Groundwater vulnerability map of the Chrzano´w karst-fissured Triassic aquifer (Poland), *Env. Geol.*, 44, 59–67, doi:10.1007/s00254-002-0735-4, 2003.
- 35 Worthington, S.R.H.: A Comprehensive strategy for understanding flow in carbonate aquifer, in: *Karst Modeling*, Proceedings of the symposium held 24-27 February, 1999 Charlottesville (Virginia), edited by: Palmer, A.N., Palmer, M.V., and Sasowsky, I.D., *Karst Waters Institute Special Publication 5*, Karst Waters Institute, Charles Town (West Virginia), 30-37, 1999.
- Zötl, J. G.: *Karsthydrogeologie*, Springer, Vienna, 291, 1974.



Tables

Table 1 Soil groups and soil properties

WRB soil group	Rendzic Leptosols	Lithic Udorthents	Chromic Cambisols	Cambisols	Luvisols	Stagnosols	Fluvic Cambisol
German soil group	Rendzina	Para-rendzina	Terra fusca	Braunerde	Para-braunerde	Pseudogley	Vega
Substratum	limestone	marlstone	limestone	marlstone, loess loam	loess loam, marlstone	loess loam, marlstone	alluvial silt+clay
Thickness	5-35 cm	15-35 cm	85-100 cm	35-80 cm	50-100 cm	80-190 cm	up to 3.3 m
Soil category (grain size)	medium silty clay	medium silty clay	slightly silty clay	medium silty clay	slightly clayey silt	medium silty clay	strongly silty clay
	Tu3-Tu4	Tu3	Tu2	Tu3	Ut2-Ut3	Ut3-Tu3	Tu4
Water storage capacity	low	low-medium	high	high	medium	very high	very high
Roots	< 35 cm	< 35 cm	30-60 cm	20-80 cm	20-180 cm	30-80 cm	15-40 cm
Cracks and borrows	earthworm borrows down to the host rock	frequent	earthworm borrows down to the host rock	frequent	deep borrows (voles, worms)	limited to shallow soil horizons	limited to shallow soil horizons
Decarbonatization	no	no	complete	almost complete	complete	incomplete	no
Typical color (subsoil)	yellowish gray	yellowish gray	dark yellowish gray	brownish gray	yellowish gray	greenish gray	yellowish gray
	10YR3/2	10 YR4/3	7,5YR4/3	10YR5/6	10YR4/6	2,5Y4/2	10YR4/3
Hydromorphic attributes	no	barely developed	oxidative	oxidative	oxidative	oxidative + reductive motteling	oxidative + reductive motteling
Soil water	> 200 cm	> 200 cm	rarely and > 80 cm	rarely and > 100 cm	rarely and > 100 cm	commonly in 1-2 m	very common > 40-60 cm
Morphologic position	middle slope + all steep local slopes	middle slope	culmination + local plateaus	culmination to middle slope	lower slope, (middle slope)	lower slope, valley	valley centre
Land use	forest + military training area	forest + military training area	forest + some grassland	cropland, grassland, forest	cropland, grassland, uncommonly forest	grassland, uncommonly forrest	grassland
Anthropogenic changes	uncommon	compacted (tanks), drained	uncommon	ploughed, compacted	ploughed, compacted	drained	drained

**Table 2** Hydrostratigraphic standard section

German time scale (DSK, 2002) [Ma]	Level above base of moTK [m]	German stratigraphy (DSK, 2002)	Regional stratigraphy (Central Germany. Seidel, 2003)	Aquifer assemblages (Küsel et al., 2016)	Aquifer storeys (this study) X aquifer - aquitard	Level above base of moTK [m]	Ground-water well (screen section)
0.01...0			soils alluvial sediments (qhf) loess (qwLo)				
0.1...0.01							
232.5...0.1					erosional unconformity		
235.0... 232.5	61.3... >90.0	Erfurt formation (kuE)	Graue Mergel (kuGM) Sandstein- komplex1 (kuS1) Grenzschichten (kuGR)		- X - X -	kuS1-2 kuS1-1	74.5...76.5 68.0...70.0
	43.4... 61.3	Warburg formation (moW)	Glasplatten (moCGP) Glaukonitbank (moCG) Zinkblendebank Fischschuppen- schichten (moCFU)		- X - -	moW-1	53.0...54.0
238.5... 235.0	8.7... 43.4	Meissner formation (moM)	Cycloidesbank (moCC) Discites- schichten (moCD) Gervilleien- schichten (moCGV)	HTU (Hainich transect upper aquifer assem- blage)	X - X - - X - - X - - X - - X -	moM-9 moM-8 moM-7 moM-6 moM-5 moM-4 moM-3 moM-2 moM-1	42.0...45.0 38.0...40.5 H42, H43, H53 34.0...36.0 H44 31.0...33.7 H32, H44 27.0...29.0 H32 22.9...24.5 H52 18.9...21.8 H52 15.2...18.3 H23 8.0...13.2 H14
>238.5	0.0... 8.7	Trochiten- kalk formation (moTK)	Trochitenkalk (moT)	HTL (lower aquifer assem- blage)	X	moTK-1	0.0...6.6 H11, H12, H13, H21, H22, H31, H41, H51



Figures

Fig. 1. Location of the Hainich CZE (a + b): Prominent karst springs in the Hainich CZE are coupled to fault zones (b; modified from Mempel, 1939 and Jordan and Weder, 1995). Monitoring wells of the research transect, accessing Upper Muschelkalk target formations, are located at the eastern Hainich hillslope (c); Data sources:

5 DEM ©GeoBasisDE/TLVermGeo, Gen.-Nr.: 7/2016.

Fig. 2. Land use types, soil groups and soil thickness classes in the subcatchment (a); pie charts (b) show relative abundances of land use types in the recharge areas of the aquifer storeys, which are sampled in our monitoring wells (chapter 3.4).

10 **Fig. 3.** Groundwater classification (Piper plot) of grouped aquifer storeys, aquifer assemblages and monitoring wells.

Fig. 4. Principal component analysis (PCA) biplot for the complete parameter set (a) and for the limited parameter set (b) without redox related parameters.

15 **Fig. 5.** Stratigraphic succession of the Upper Muschelkalk with the aquifer storeys moTK-1 to moM-9 and average chemical compositions of monitored groundwaters.

Fig. 6. Correlation of gamma-ray logs, biostratigraphic limestone marker beds and the degree of karstification (red bars). The geological aquifer correlation is cross-checked with the hierarchical clustering of hydrochemical parameters.

20

Fig. 7. Average groundwater chemistry of clusters 1-5.

Fig. 8. Outcrop zones of all aquifer storeys, surface karst phenomena, groundwater isolines and rivers. The conceptual cross section shows the overall geological structure with aquifer storeys, soil groups, land use types, and fault/karstification zones (potential groundwater mixing); Data sources: DEM ©GeoBasisDE/TLVermGeo, Gen.-Nr.: 7/2016.

25



Fig. 1.

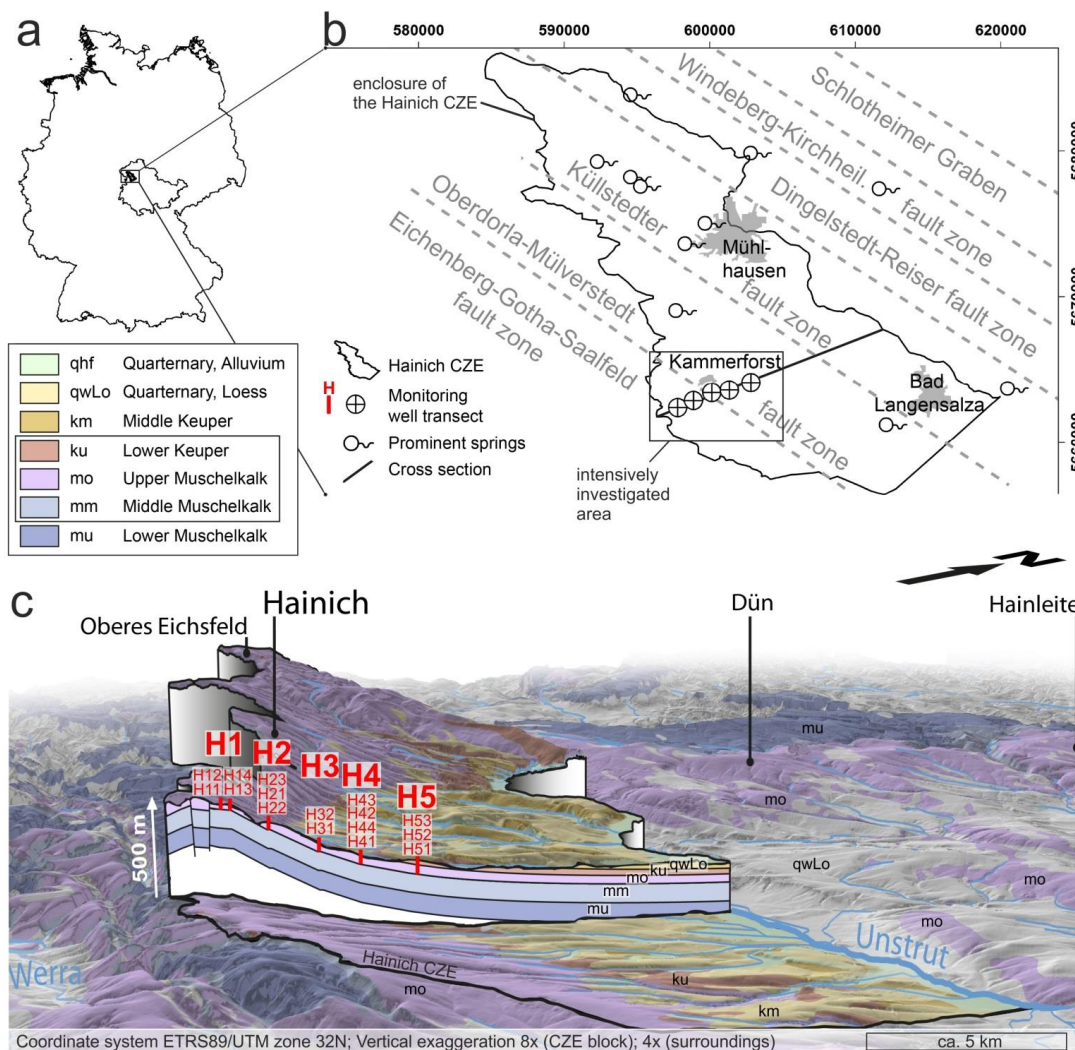


Fig. 1. Location of the Hainich CZE (a + b); Prominent karst springs in the Hainich CZE are coupled to fault zones (b; modified from Mempel, 1939 and Jordan and Weder, 1995). Monitoring wells of the research transect, accessing Upper Muschelkalk target formations, are located at the eastern Hainich hillslope (c); Data sources: DEM ©GeoBasisDE/TLVermGeo, Gen.-Nr.: 7/2016.



Fig. 2.

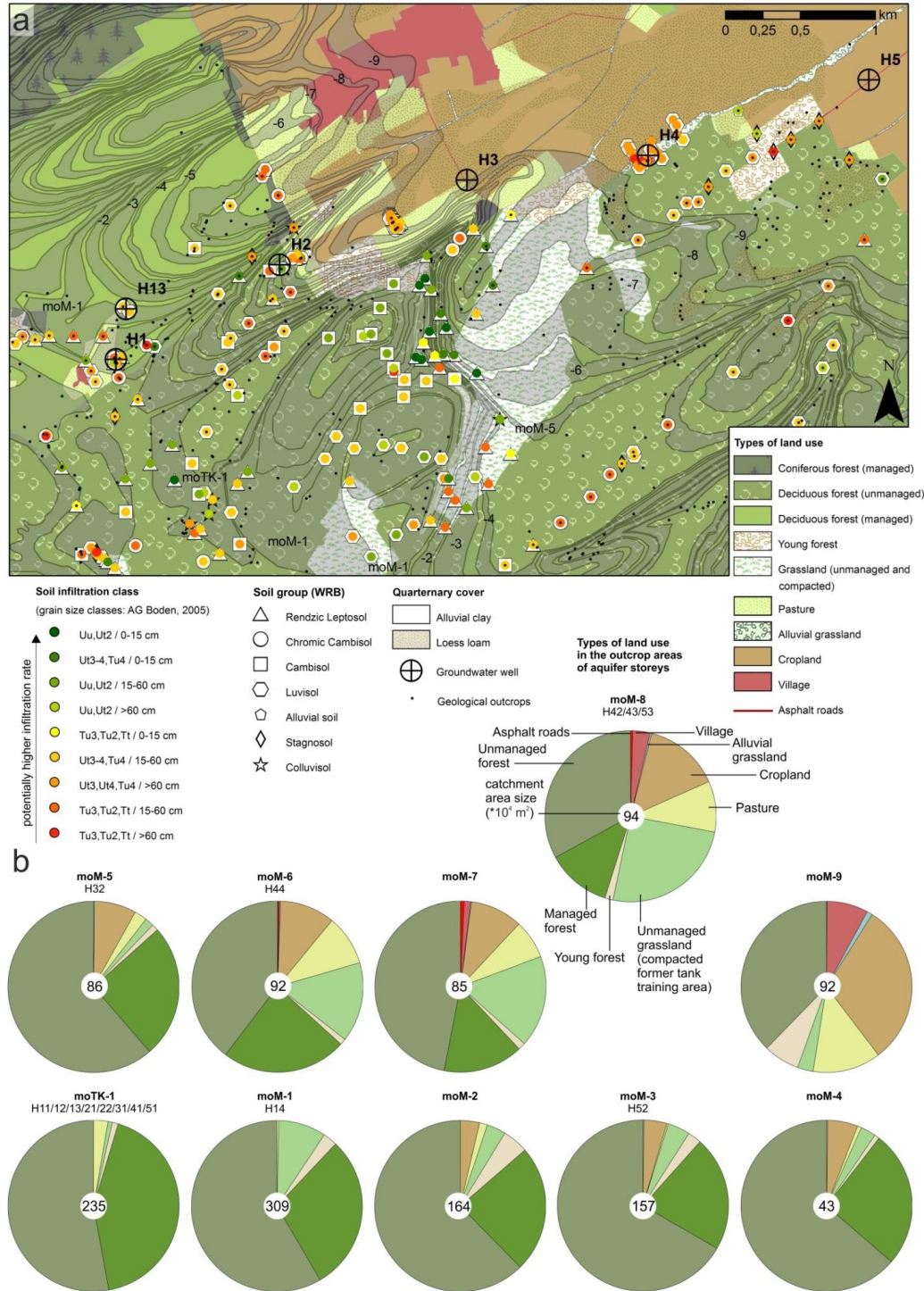


Fig. 2. Land use types, soil groups and soil thickness classes in the subcatchment (a); pie charts (b) show relative abundances of land use types in the recharge areas of the aquifer storeys, which are sampled in our monitoring wells (chapter 3.4).



Fig. 3.

Classification

(Furtak and Langguth, 1967)

- a earthalkaline waters, predominantly bicarbonatic
- b earthalkaline waters, bicarbonatic-sulfatic
- c earthalkaline waters, predominantly sulfatic

Subtypes

(Kralik et al., 2005)

predominantly in contact with:

- h CaCO_3
- j CaCO_3 and $\text{CaMg}(\text{CO}_3)_2$
- k $\text{CaMg}(\text{CO}_3)_2$

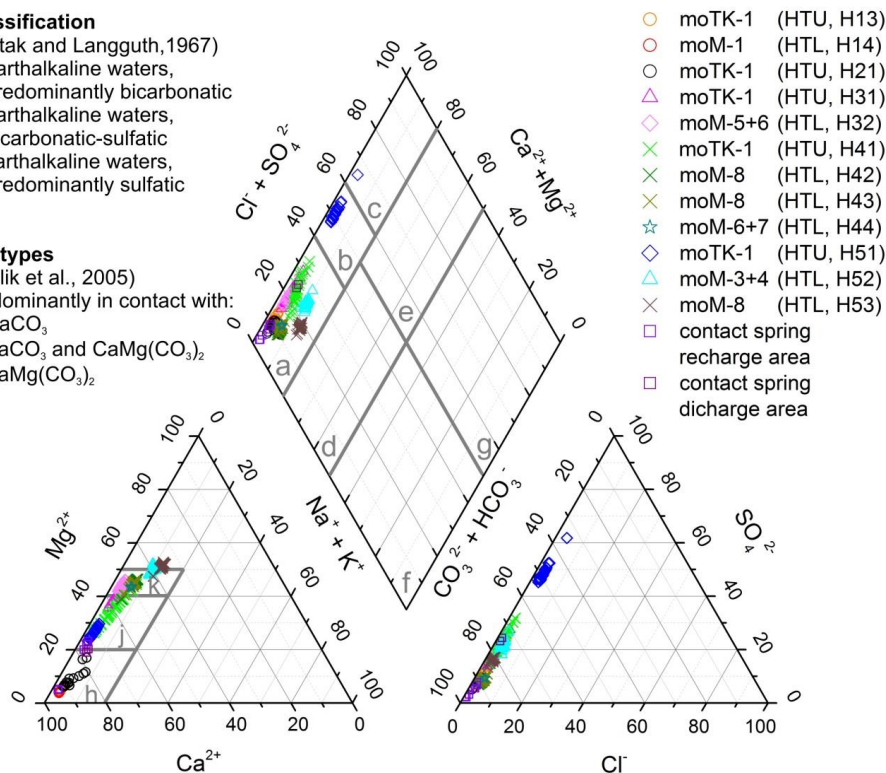


Fig. 3. Groundwater classification (Piper plot) of grouped aquifer storeys, aquifer assemblages and monitoring wells.



Fig. 4.

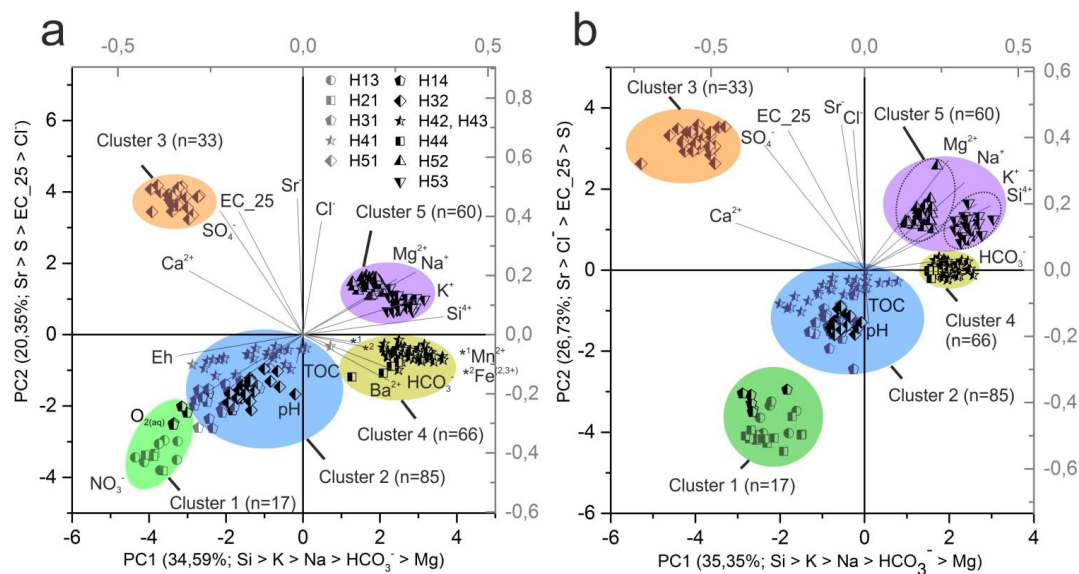


Fig. 4. Principal component analysis (PCA) biplot for the complete parameter set (a) and for the limited parameter set (b) without redox related parameters.

5



Fig. 5.

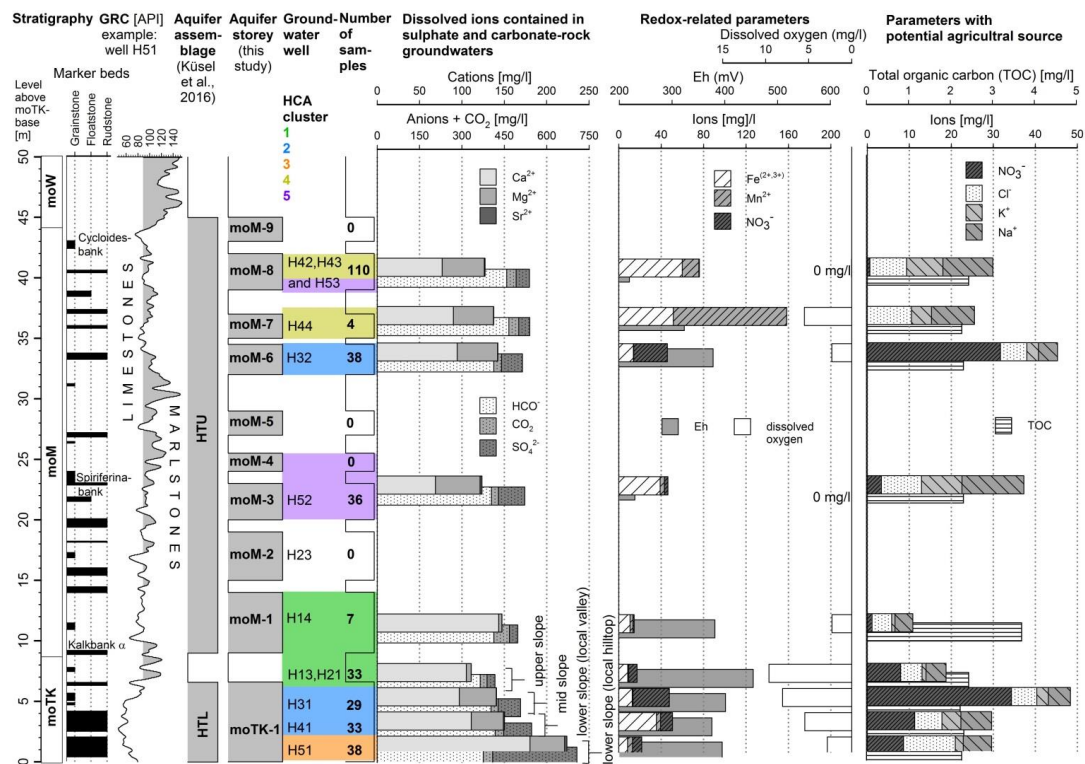


Fig. 5. Stratigraphic succession of the Upper Muschelkalk with the aquifer storeys moTK-1 to moM-9 and average chemical compositions of monitored groundwaters.

5



Fig. 6.

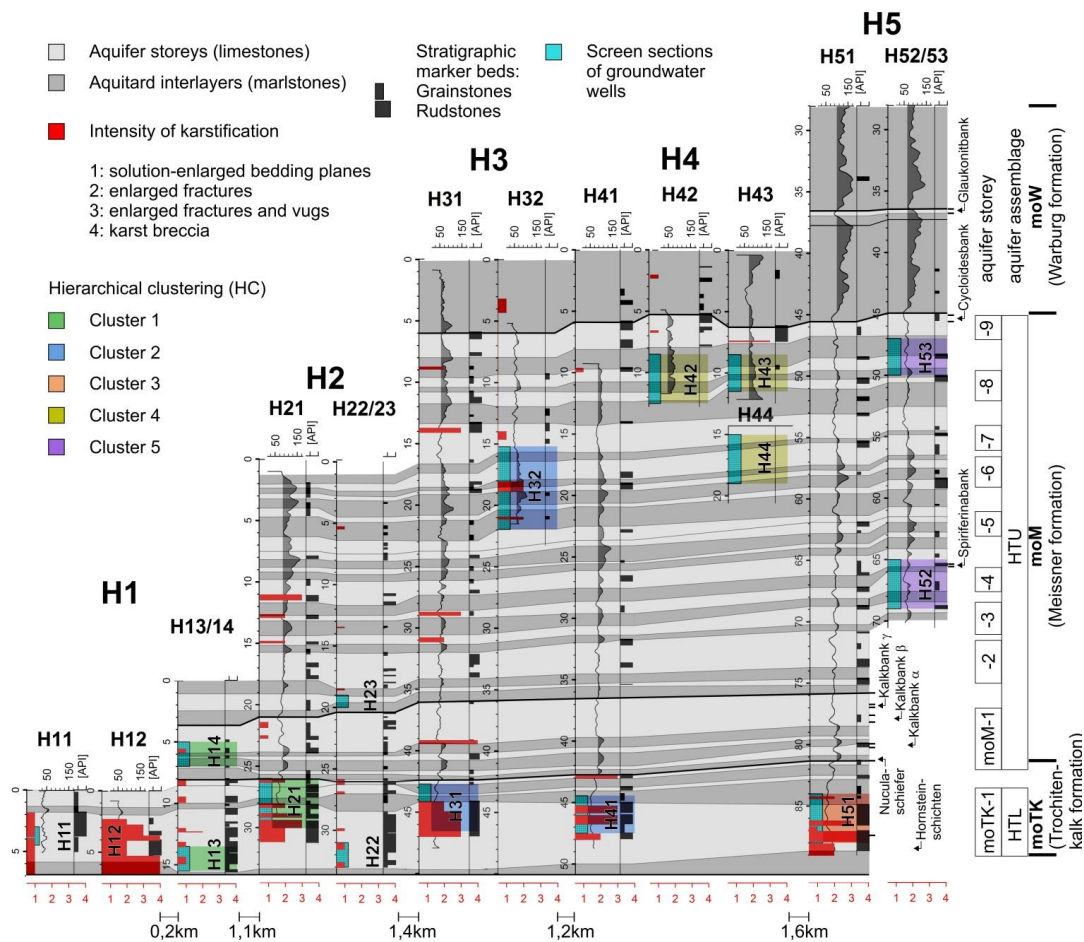


Fig. 6. Correlation of gamma-ray logs, biostratigraphic limestone marker beds and the degree of karstification (red bars). The geological aquifer correlation is cross-checked with the hierarchical clustering of hydrochemical parameters.

5



Fig. 7

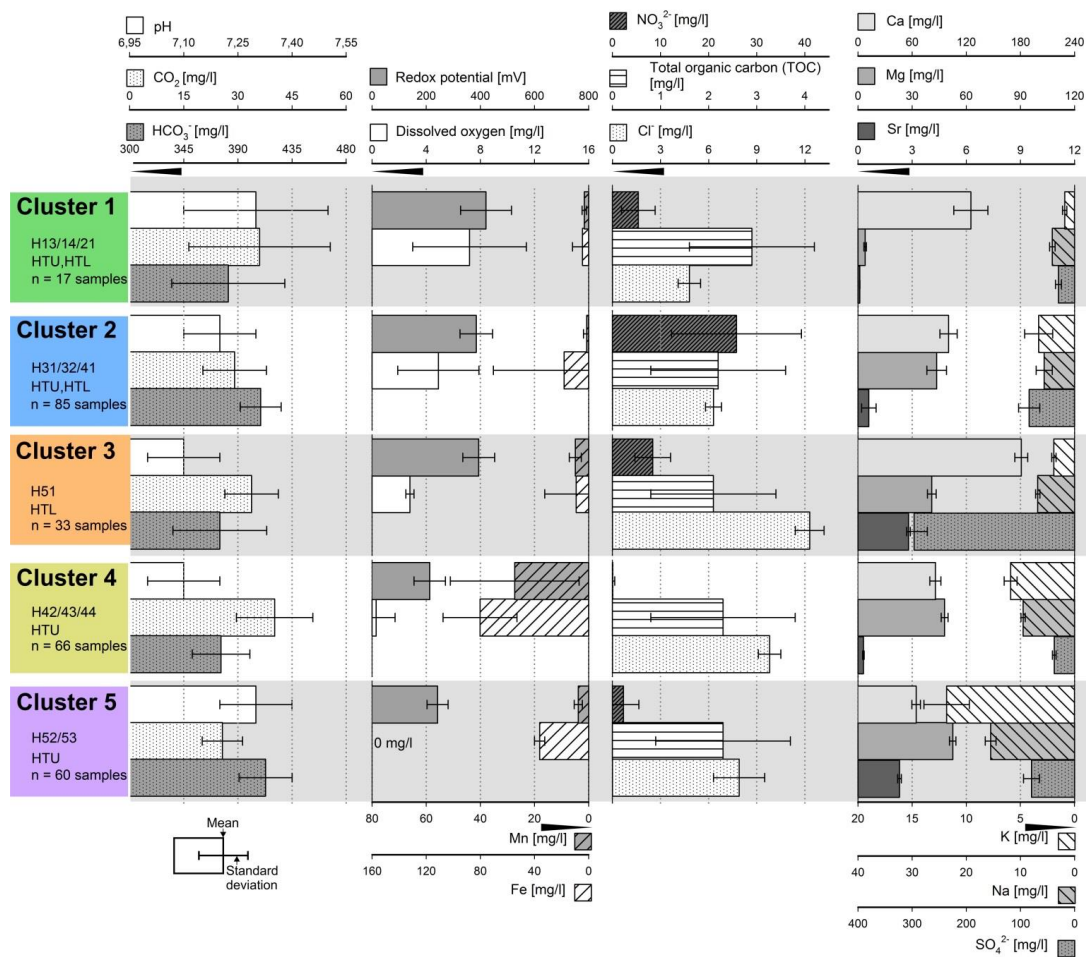


Fig. 7. Average groundwater chemistry of clusters 1-5.



Fig. 8.

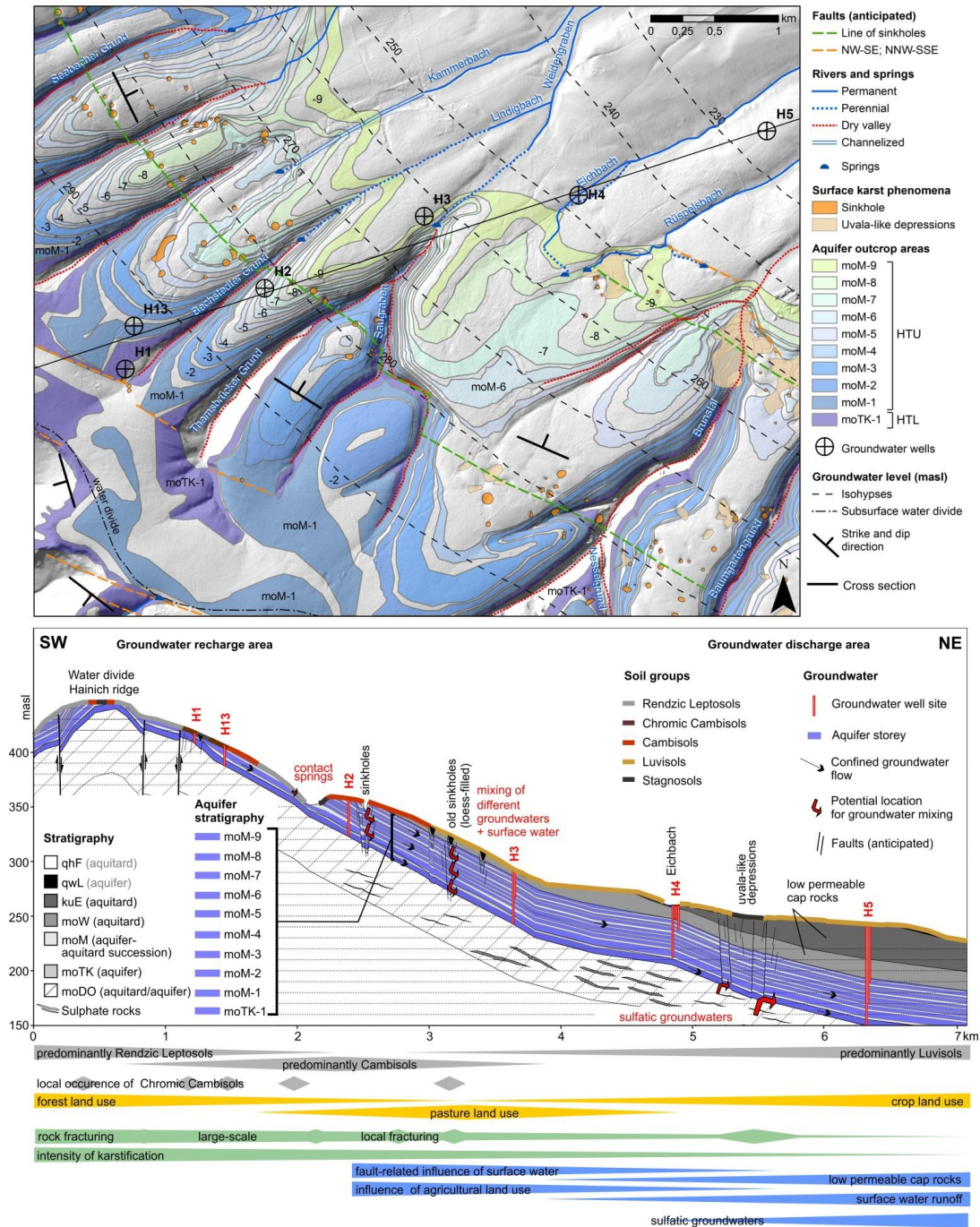


Fig. 8. Outcrop zones of all aquifer storeys, surface karst phenomena, groundwater isolines and rivers. The conceptual cross section shows the overall geological structure with aquifer storeys, soil groups, land use types, and fault/karstification zones (potential groundwater mixing); Data sources: DEM ©GeoBasisDE/TLVermGeo, Gen.-Nr.: 7/2016.

5